

Variable stars in the open cluster NGC 6791 and its surrounding field^{*}

F. De Marchi¹, E. Poretti², M. Montalto¹, G. Piotto¹, S. Desidera³, L. R. Bedin⁴,
R. Claudi³, A. Arellano Ferro⁵, H. Bruntt⁶, and P. B. Stetson⁷

¹ Dipartimento di Astronomia, Università di Padova, Vicolo dell'Osservatorio 2, 35122, Padova, Italy
e-mail: fabrizio.demarchi@unipd.it

² INAF - Osservatorio Astronomico di Brera, via E. Bianchi 46, 23807 Merate (LC), Italy

³ INAF - Osservatorio Astronomico di Padova, Vicolo dell'Osservatorio 5, 35122, Padova, Italy

⁴ Space Telescope Science Institute, 3700 San Martin Drive, Baltimore, MD 21218, USA

⁵ Instituto de Astronomía, Universidad Nacional Autónoma de México, DF, Mexico

⁶ School of Physics A28, University of Sydney, NSW 2006, Australia

⁷ Herzberg Institute of Astrophysics, Victoria, Canada

Received 1 March 2007 / Accepted 12 June 2007

ABSTRACT

Aims. This work presents a high-precision variability survey in the field of the old, super metal-rich open cluster NGC 6791.

Methods. The data sample consists of more than 75 000 high-precision CCD time series measurements in the *V* band obtained mainly at the Canada-France-Hawaii Telescope, with additional data from S. Pedro Mártir and Loiano observatories, over a time span of ten nights. The field covers an area of 42×28 arcmin².

Results. We have discovered 260 new variables and re-determined periods and amplitudes of 70 known variable stars. By means of a photometric evaluation of the membership in NGC 6791, and a preliminary membership based on the proper motions, we give a full description of the variable content of the cluster and surrounding field in the range $16 \lesssim V < 23.5$. Accurate periods can be given for the variables with $P \lesssim 4.0$ d, while for ones with longer periods the limited time-baseline hampered precise determinations. We categorized the entire sample as follows: 6 pulsating, 3 irregular, 3 cataclysmic, 89 rotational variables and 61 eclipsing systems; moreover, we detected 168 candidate variables for which we cannot give a variability class since their periods are much longer than our time baseline.

Conclusions. On the basis of photometric considerations, and of the positions of the stars with respect to the center of the cluster, we inferred that 11 new variable stars are likely members of the cluster, for 22 stars the membership is doubtful and 137 are likely non-members. We also detected an outburst of about 3 mag in the light curve of a very faint blue star belonging to the cluster and we suggest that this star could be a new U Gem (dwarf nova) cataclysmic variable.

Key words. stars: starspots – stars: statistics – stars: variables: general – stars: binaries: eclipsing – stars: novae, cataclysmic variables – open clusters and associations: individual: NGC 6791

1. Introduction

The photometric precision achieved by several ongoing transiting planet searches allows us to extend the census of variable stars down to very low amplitudes and faint magnitudes in selected sky regions. Variable stars are an important source of astrophysical information: from observations of them we are able to test several theories (e.g., evolutionary and pulsational models). Since all stars in an open cluster have essentially the same age, chemical composition and distance, the study of variables which are cluster members can put more severe constraints on the physical parameters. Comparisons can also be made between the variable stars of the cluster and those of the surrounding field.

In this paper, we present the study and the classification of 260 new variable stars that we found in the field of the open cluster NGC 6791, while for 70 already known variables we compare our results with the previous ones. NGC 6791 ($\alpha = 19^{\text{h}}20^{\text{m}}53^{\text{s}}$; $\delta = +37^{\circ}46'18''$), is a rich and well studied open cluster. It is thought to be the one of the oldest and probably

the most metal-rich cluster known in our Galaxy. Its age is estimated to be about 8–9 Gyr (Carraro et al. 2006; King et al. 2005; Chaboyer et al. 1999; Stetson et al. 2003; Kaluzny & Rucinski 1995); however, the white dwarf cooling sequence indicates a different value, i.e., ~ 2.4 Gyr (Bedin et al. 2005). The most recent estimates of its metallicity are $[\text{Fe}/\text{H}] = +0.39$ (Carraro et al. 2006), $[\text{Fe}/\text{H}] = +0.47$ (Gratton et al. 2006), and $[\text{Fe}/\text{H}] = +0.45$ (Anthony-Twarog et al. 2006). In this work we adopt for NGC 6791 a distance modulus $(m - M)_V = 13.35 \pm 0.20$ mag and a reddening $E(B - V) = 0.09$ mag (Carraro et al. 2006). The cluster is thus located at about 4.1 kpc from the Sun.

Because of its extreme characteristics, NGC 6791 has been the target of many surveys (see Table 1 for a list of publications). Taking into account the fact that in four cases the same stars have two identification numbers (V15 \equiv B7, V56 \equiv V96, V76 \equiv V85 and V77 \equiv V88) and counting also the stars B4 and B8, the total number of known variable stars in the field of NGC 6791 to date was 123 (plus 7 suspected variables, proposed by Hartman et al. 2005).

In Sect. 2 below we describe our observations, in Sect. 3 we give details about the methods we employed in the search for

^{*} Appendix A is only available in electronic form at <http://www.aanda.org>

Table 1. Previous variable star searches in NGC 6791.

Authors	Nr. of variables	IDs	Notes
Kaluzny & Rucinski (1993) (KR93)	17	V1–V17	V15 \equiv B7
Rucinski et al. (1996) (RK96)	5	V18–V21 and B8	
Mochejska et al. (2002) (M02)	47	V22–V67 and B4	B4 was previously catalogued by Kaluzny & Udalski (1992) as a blue star, but not as variable.
Mochejska et al. (2003) (M03)	7	V68–V74	
Kaluzny (2003) (K03)	4	V75–V78	
Bruntt et al. (2003) (B03)	19	V79–V100	V85 \equiv V76; V56 \equiv V96; V77 \equiv V88
Mochejska et al. (2005) (M05)	14	V101–V114	
Hartman et al. (2005)	10	V115–V124	Plus 7 suspected variables

variable stars, which are themselves presented in Sect. 3.2. In Sect. 4 we describe the properties of the variable stars, focusing our attention on probable cluster members and some additional peculiar cases. The entire catalogue of variable stars is reported in an Appendix.

2. Observations and data reduction

We surveyed NGC 6791 to detect the transits of extrasolar planets (Montalto et al. 2007). The campaign covered 10 consecutive nights (from July 4, 2002 to July 13, 2002) and it was characterized by the continuous monitoring of the target on each clear night. Therefore, in addition to the planetary transit search, we could get access to the full variability content at $P \lesssim 4.0$ d, both for the cluster and the surrounding field. Three telescopes were used:

1. the Canada-France-Hawaii Telescope (CFHT) in Hawaii equipped with the CFHT12k detector, composed of 12 CCDs of 4128×2048 pixels and covering a field of about 0.32 deg^2 . Owing to the large number of bad columns, data from chip 6 could not be used, so we could get data over a 0.29 deg^2 field;
2. the San San Pedro Mártir (SPM) 2.1-m telescope equipped with the Thomson 2k detector and covering a field of about $6 \times 6 \text{ arcmin}^2$;
3. the Loiano 1.5-m telescope equipped with BFOSC + the EEV 1300 \times 1348B detector and covering a field of $11.5 \times 11.5 \text{ arcmin}^2$.

Table 2 gives details about the length of the observing nights while Fig. 1 shows the field of the CFHT survey and the edges of the Loiano and SPM surveys. The coordinates of the edges of our fields are also listed in Table 2. The field of the SPM observations is entirely included within chip 9 and the field of the Loiano observations partially covers chips 2, 3, 4, 8, 9 and 10 of CFHT (see Fig. 1). The luminosities of the new variables range from $V = 23.2 \text{ mag}$ to $V \sim 16 \text{ mag}$ (near 1 mag above the turn-off); brighter stars are saturated. The calibration of the CFHT, Loiano and SPM data have been performed by using the Kaluzny & Rucinski photometry (1995). More details on the data reduction procedure can be found in Montalto et al. (2007).

3. The identification of variable stars

The intensive monitoring of NGC 6791 allowed us to obtain tens of thousands of photometric time series for stars located in, close to, and far away from the cluster center. We have analysed 73331, 6055, and 2152 light curves obtained from the CFHT, Loiano and SPM telescopes respectively. The CFHT,

Table 2. The observation log for each night and the limits of the field of view at the 3 different observatories.

Night	Loiano		SPM		CFHT	
	t_{start} (HJD-2 452 400)	t_{end}	t_{start} (HJD-2 452 400)	t_{end}	t_{start} (HJD-2 452 400)	t_{end}
1st					59.82	59.96
2nd					60.83	61.02
3rd	62.48	62.63	61.68	61.95	61.94	62.07
4th	63.41	63.63	62.68	62.96	62.76	63.07
5th	64.38	64.64	63.68	63.96	63.88	64.10
6th	65.39	65.62	64.69	64.98	64.77	65.11
7th			65.70	65.82		
8th			66.69	66.97		
9th			67.67	67.98	67.77	68.10
10th			68.69	68.87	68.76	69.11
α_{min}	19 ^h 20 ^m 25 ^s .8		19 ^h 20 ^m 36 ^s .3		19 ^h 19 ^m 23 ^s .7	
α_{max}	19 ^h 21 ^m 30 ^s .4		19 ^h 21 ^m 10 ^s .4		19 ^h 22 ^m 58 ^s .0	
δ_{min}	37°41′22″.6		37°43′15″.4		37°36′6″.7	
δ_{max}	37°53′42″.7		37°50′3″.1		38°4′21″.2	

Loiano and SPM time series are composed of about 250, 60 and 170 datapoints, respectively. The observations, intended to detect photometric transits, were performed in the V band only.

3.1. The search for variable candidates

To search for variable stars, we calculated the best “sinusoid plus constant” fit for all light curves (Vanicek 1971; Ferraz-Mello 1981). We evaluated the goodness of the fit by calculating parameters related to the reduction of the initial variance obtained by introducing the periodic term. These parameters are the reduction factor (Vanicek 1971) and the coefficient of spectral correlation $S(\nu)$ (Ferraz-Mello 1981).

Owing to the huge number of light curves, we need one or more parameters to discover the variability. Toward this goal, we considered the parameter r defined as $r = \log_{10} S_{\text{max}}$, where S_{max} is the maximum value of S (i.e., the one corresponding to the frequency of the best-fit sinusoid in the Ferraz-Mello method). If a star does not show variability the introduction of a sinusoid does not improve the fit and then S_{max} is close to zero (no variance reduction) and $r \ll 0$; on the other hand, a sine-shaped variability strongly reduces the variance (S close to 1) and hence $r = 0$. The purpose was to use the r parameter as a tracer of variability for short-period (i.e., intranight) variability.

To search for long-period variability, we introduced a second parameter, more sensitive to the night-to-night variations. We calculated the mean magnitude V_i and the standard

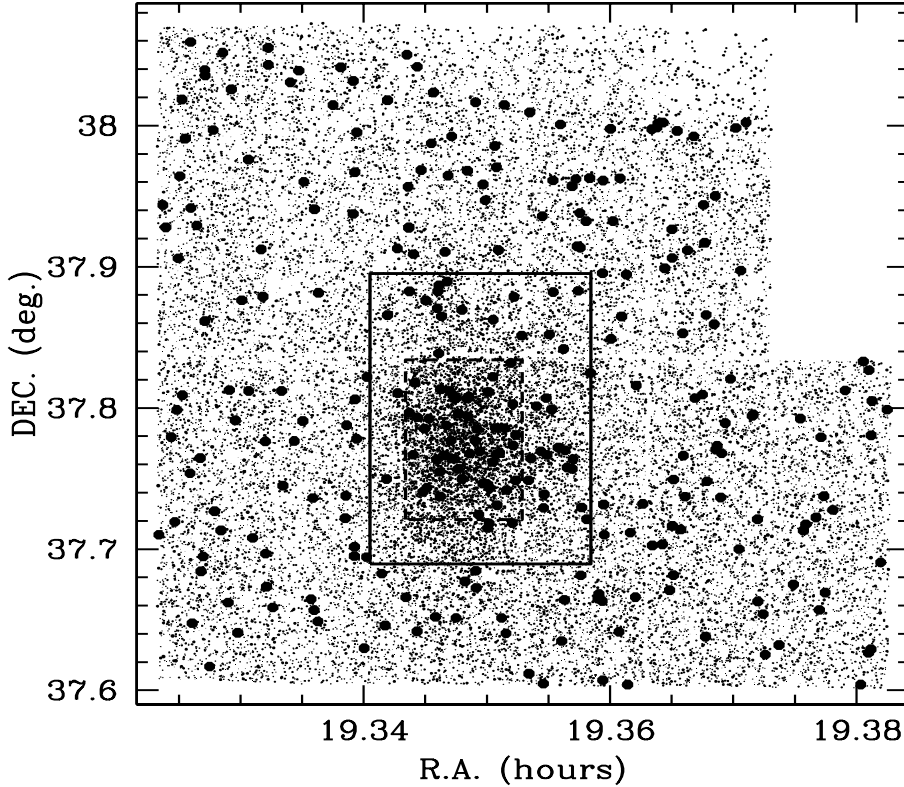


Fig. 1. Field of view (42×28 arcmin²) of the CFHT image. The chips are numbered in increasing order from left to right from chip 1 (*top left*) to chip 12 (*bottom right*); stars of chip 6 are not plotted since we found it impossible to derive accurate photometry. Dashed and solid lines are the edges of the SPM and Loiano fields, respectively. Variable stars are also plotted: *blue dots* are pulsating variables, *purple dots* are irregular and cataclysmic variables, *green dots* and *cyan dots* are eclipsing systems (EA/EB-type and EW-type, respectively). Finally, *red* and *yellow dots* are rotational and long-period variables, respectively.

deviation σ_i on each night, and after that we calculated the parameter s defined as:

$$s = \log_{10} \frac{\Delta V}{\bar{\sigma}}$$

where ΔV is the peak-to-peak difference and $\bar{\sigma}$ is the mean of the σ_i over all nights.

To test the capability of the r and s parameters to detect variable stars, we prepared a sample containing two types of light curves: 7722 artificial *constant* light curves (see Montalto et al. 2007, for details) and 70 light curves of *already known variable stars* which are included in our CFHT field. In Fig. 2 we plot r vs. s for the light curves of constant stars (small points) and of variable stars (large points). The variable stars are substantially apart from the constant stars and most have $r \gtrsim -1$. The variable stars with $r \lesssim -1$ and superposed on constant stars are mostly EA-type stars or irregular stars (e.g., cataclysmic variables). Among variables (i.e., large dots in Fig. 2), the stars with small s have short periods ($P \leq 0.50$ d), while stars with large s have long periods. Therefore, we can conclude that the combination of the r and s parameters is a good tracer of variability.

To detect the variable stars in our sample of $\sim 82\,000$ light curves we first selected in an automatic way all the stars with $r \geq -2.0$, according to the test described above. We thereby reduced the huge initial sample to $\sim 6\,500$ stars. After the calculation of the amplitude spectrum of their time series, we adopted as a second selection criterion a signal-to-noise ratio (S/N) greater than 4.0 around the highest peak in the amplitude spectrum. This procedure allowed us to reduce our sample to ~ 900 stars, i.e., 1.1% of the whole initial sample. Further checks have been made by examining the light curves of a random sample of stars with $r < -2.0$, large s and $3.5 < S/N < 4.0$, but we did not find any additional variables.

Our approach allowed us to detect hundreds of stars showing peaks in their power spectra at $f = 1.00$ cd⁻¹, at

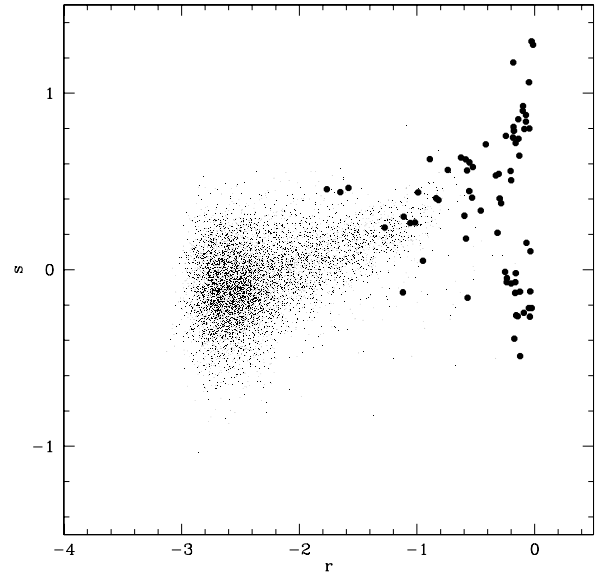


Fig. 2. *Grey points*: r parameter vs. s parameter for constant light curves. *Black dots*: parameters derived from our light curves for the variable stars previously detected in our field.

$f \leq 0.05$ cd⁻¹, or at $f = 0.6$ cd⁻¹. The first two spurious periodicities are common and can be ascribed to small misalignments in the mean magnitudes from one night to the next or recurrent drifts (caused by small color effects, for example) in the intranight light curves. We suggest that the latter one is probably a photometric artefact occurring in some particular cases of blended stars, or stars close to CCD edges, or bad pixels. They have been considered as not reliable enough to infer a physical light variability. In our opinion, only the combination of automatic procedures and visual inspection allowed us to identify the three classes ($P = 1.00$ d, $P = 1.6$ d, $P \gg 10$ d) of spurious

variables in the huge number of $\sim 82\,000$ light curves. In particular, we note that the identification of the whole sample of eclipsing binaries has been confirmed by the application of the box fitting technique (BLS, Kóvács et al. 2002), used by Montalto et al. (2007) to detect planetary transits.

At the end of the variable star identification, we were left with 330 cases to be characterized. Since we rejected about 2/3 of the sample selected by means of the r, s parameters, we are confident we have not applied overly strict constraints in the candidate selection.

3.2. The cross check with previous surveys of NGC 6791

When comparing our field of view with those of other surveys, we found that 81 known variable stars are included. The CFHT survey failed to detect 45 known variable stars: seventeen stars (V22, V24, V26, V28, V30, V35, V36, V47, V50, V57, V61, V63, V64, V102, V103, V104, V105) are outside the CFHT field of view; 4 stars (V71, V106, V113 and V120) lie between two chips; 23 stars (V1, V6, V13, V19, V33, V39, V45, V49, V54, V56 \equiv V96, V65, V66, V67, V69, V70, V72, V73, V74, V77 \equiv V88, V78, V81, V97 and V112) are saturated; and the V76 data are useless.

Among the 81 known variable stars that we have observed, not all of them display variability in our sample: 4 stars (V10, V18, V21, V32) are previously classified as long-period detached eclipsing variables and we did not observe eclipses. We are not able to confirm the period of 15.24 days for V68 (M03), likely because of our shorter time baseline and the small amplitude of this variable (about 0.003 mag in V -band, M03). Finally, we cannot confirm the variability of six stars (V20, V79, V84, V98, V99, V116) and of the seven suspected variables found by H05, since our data do not show any trace of variability.

Among the sample of the stars missing from the CFHT field, we identified 22 stars in the Loiano and SPM data sets (V6, V13, V19, V20, V33, V45, V54, V56 \equiv V96, V65, V66, V67, V70, V71, V73, V74, V76 \equiv V85, V77, V78, V81, V97, V106 and V113). However, owing to the smaller signal-to-noise ratio (S/N), the small number of datapoints and (in the case of the Loiano data) the limited survey time, we could only confirm the variability of stars V56 \equiv V96, V66 and V76 \equiv V85.

Throughout this paper we use the existing names for the already known variables; to identify the new ones discovered in our survey we used the five-digit number assigned by the DAOPHOT package followed by the number of the chip which the star belongs to. Accurate astrometry is provided to identify the stars on the sky. Moreover, all light curves of the variables will be available on CDS.

4. The variable star content of NGC 6791 and its surrounding field

The CFHT measurements are quite precise, thus the light curves are generally very well defined for $P < 4$ d. On the other hand, the periods and the shapes are uncertain for $P > 4$ d, since the observations only covered 2.5 cycles or less. We refer to Montalto et al. (2007) for a full description of the photometric errors. In order to evaluate the precision in the study of the variable stars, we calculated the standard deviations of the Fourier least-squares fits (truncated at the last significant term for the given star) for the 138 light curves having very good phase coverage. The precision was found to be better than 0.010 mag in 73 cases (53%), and better than 0.020 mag in a total of 122 cases (88%),

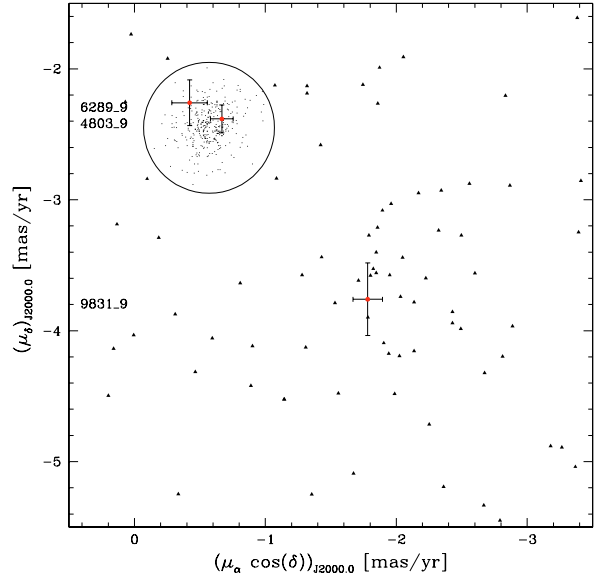


Fig. 3. Proper-motion vector-point diagram for the inner region of NGC 6791 (from Bedin et al. 2006). The circle (centered on the absolute proper motion of the cluster) represents a safe limit corresponding to 0.5 mas/yr. Triangles represent non-members, points with error bars are the new variables 06289_9, 04803_9 and 09831_9.

as expected for stars ranging from $V \sim 16.0$ to $V \sim 22.5$. The discussion based is mostly on the CFHT data, which are by far the most numerous, precise and homogeneous; however, for some variables we have used data from Loiano and SPM in a very profitable way. As an example, only the longitude spread of the three observatories allowed us to derive the periods of the eclipsing binaries 00645_10, V107, V12, V109 and of the rotational variable 03079_9.

To proceed in the definition of the variable star content of NGC 6791 and its surrounding field, we calculated the power spectra of the data for all the 330 candidate variables by using the least-squares iterative sine-wave search (Vanicek 1971) and the Phase Dispersion Minimization (Stellingwerf 1978) methods. Differences have been examined and resolved. The separation into different classes of variable stars has been made on the basis of the light curve parameters (period, amplitude, Fourier coefficients) and standard photometric values ($V, B - V, V - I$), when available. The period estimates have been refined by means of a least-squares procedure (MTRAP, Carpino 1987) and appropriate error bars have also been calculated. At the end of the process we get six pulsating stars with $P < 0.6$ d, three irregular variables, three cataclysmic variables (CVs), 31 detached or semi-detached eclipsing binaries, 29 contact binaries, 90 rotational variables, 167 stars showing clear night-to-night variability on timescales too long for periods to be determined over our 9.2-d baseline. We adopt preliminary membership probabilities based on proper motion measurements kindly provided to us by K. Cudworth (private communication) for 35 stars. Moreover, for three new variable stars we adopted membership probabilities based on proper motions performed by Bedin et al. (2006) (hereafter B06, see Fig. 3).

For the other stars, we consider their position in color-magnitude diagrams (CMDs), and their distance from the center of the cluster to infer whether they belong to the cluster (for EW-type stars we also utilize the P - L - C relation of Rucinski (2003)). Toward this end, we plotted the radial distribution of all stars in Fig. 4. We see that at a distance of $\sim 10'$ from the center

Table 3. Pulsating, irregular and cataclysmic variables. V is the minimum brightness for CVs and irregular, the mean brightness for pulsating variables. T_0 is the time of maximum brightness for pulsating stars. Hereafter, the labels “k” and “s” indicate that the $B - V$ color index is taken from Kaluzny & Rucinski (1995) or Stetson et al. (2003), respectively.

Star	Type	α_{2000}	δ_{2000}	V [mag]	$\langle B - V \rangle$ [mag]	$\langle V - I \rangle$ [mag]	Ref.	T_0 [HJD-2 452 400]	Period [d]	Ampl. [mag]
Pulsating variables										
V123	HADS	19.362064	37.666034	17.08	0.45		k	59.559	0.06026	0.14
01497_12	HADS	19.379083	37.812419	16.06				59.528	0.07227	0.40
00311_7	SXPhe	19.324628	37.716768	23.17				59.605	0.10443	0.10
00224_10	SXPhe	19.353639	37.710163	21.72	0.71	1.06	s	59.801	0.12261	0.20
03653_3	RRc	19.347147	37.992413	17.21	0.57	0.58	k	59.937	0.32654	0.39
00345_1	RRab	19.325082	37.964170	18.28				60.151	0.57866	0.72
Irregular variables										
V92	IRR	19.350754	37.766876	18.10	0.91		k			0.10
V83	IRR	19.346220	37.737232	19.10	1.02	1.05	k			0.07
V93	IRR	19.351452	37.785687	18.12	0.98	1.03	s			0.04
Cataclysmic variables										
V15(=B7)	CV	19.352057	37.799019	18.26	0.20		k			0.06
B8	CV	19.343262	37.747833	20.64	-0.23	0.78	k			2.27
06289_9	CV (?)	19.348976	37.770355	22.80	0.25	0.88	s			3.10

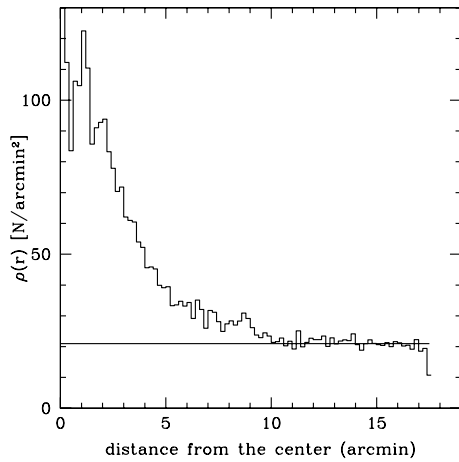


Fig. 4. Stellar density ρ (number of stars per square arcminute) as a function of the distance from the center. The straight line represents the mean stellar density at distances greater than $10'$.

of the cluster, the stellar density becomes near constant (about 21 star/arcmin²). Thus, we adopt the value of $10'$ as the external limit of the cluster and we consider “likely non-members” the variables located farther from the cluster center.

4.1. Pulsating variables

The main characteristics of our variables are listed in Table 3 and their light curves are shown in Fig. 5. The classification as High-Amplitude Delta Sct (HADS), SX Phe, RRc or RRab stars is based on the parameters of the Fourier decomposition (Poretti 2001). In all cases, the ϕ_{21} Fourier parameters are on the progressions described by the different classes. We note that our period for V123 is quite different from that given by H05 (0.107 d). Error bars on the periods are in the range $1-6 \times 10^{-5}$ d.

Both RR Lyr variables are too faint to belong to NGC 6791. Since they have $V = 17.21$ (03653_3) and $V = 18.28$ (00345_1), their distance moduli greatly exceed that of the cluster.

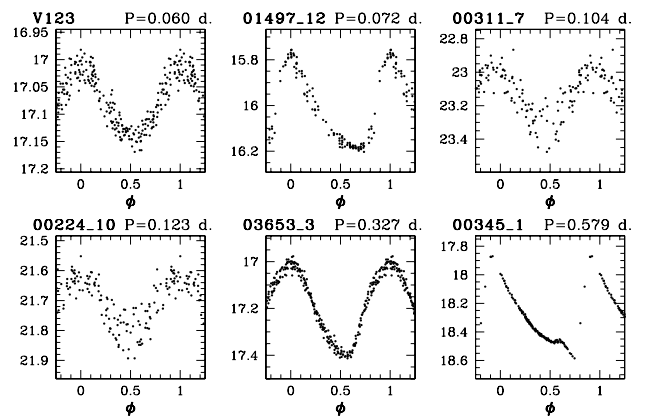


Fig. 5. Light curves of pulsating variables. V123 and 01497_12 are probably HADS stars, 00311_7 and 00224_10 are SX Phe stars, 03653_3 and 00345_1 are RR Lyr stars.

This is also true for the very faint and short-period stars 00311_7 ($V = 23.17$) and 00224_10 ($V = 21.72$); therefore, it is more likely that they are Pop. II stars. On the other hand, using the $P - L$ relation given by McNamara (2000), we get distance moduli of 14.50 and 13.78, respectively, for V123 and 01497_12. These distance moduli and the distance from the cluster center ($12'$ and $22'$, respectively) suggest that they do not belong to the cluster, though they are not very far from it. Therefore, they are probably Pop. I stars and hence High Amplitude δ Scuti stars.

Moreover, there are several variables whose light curves are very similar to those of Cepheid variables; the Fourier decomposition of some light curves (in particular the large amplitude ones, i.e., 00913_5, 01659_8, V46 and 01431_10, but also 01606_11, 02285_10, 00122_4 and 03056_3) yields parameters typical for Cepheid light curves. However, most of these variables are quite faint and the Period-Luminosity relation for Cepheids (Tammann et al. 2003) yields distances in the range 39–171 Kpc. It is difficult to say whether these stars are nearby rotational variables (see below) in the Milky Way or very

distant pulsating variables. For our present purposes, these stars have been included among the rotational variables listed in the Appendix.

The puzzling nature of all these apparently distant stars (i.e., the Cepheid-like ones, the RR Lyr and the faint SX Phe variables discussed above) deserves further investigation by means of spectroscopic and/or kinematic data.

4.2. Irregular variables

Table 3 also lists three irregular variables: these stars lie on the middle Main Sequence and are all located less than $3'$ from the cluster center; thus we suggest that they belong to the cluster. V92 and V83 were previously defined as “periodic variables” by B03. Indeed, we noticed fast variability in our light curves (Fig. 6), but, more noticeably, the mean magnitude is also changing from night to night. The long periods given by M03 are not able to explain either the short- or the longer-timescale variability; actually, we could not detect any periodic term. We also detected no trace of periodicity in V93 (Fig. 6); we suspect that the periods given by M05 and B03 are spurious, since they are close to 1.0 d (0.99 and 0.94 d, respectively) and they could be produced by the irregular fluctuations.

We can conjecture that these variables are eruptive variables observed in a quiescent phase, in which rapid and/or slow changes with smaller amplitude can be observed; they resemble the case of V15 (see Sect. 4.3). We have no reliable indications about the membership probabilities.

4.3. Cataclysmic variables

As regards V15: M03 and M05 detected variability over the range of 3 mag and observed outbursts of about 0.5–1.0 mag; from our side, we could see a 0.15-mag variability in our light curves (Fig. 6), corresponding to the quiescent phase. V15 is very probably a NGC 6971 member, since the Cudworth proper-motion membership probability is very high (98%).

Both the position of the faint blue star 06289_9 in the two-colour diagram and the shape of its light curve (Fig. 7) strongly suggest that this star could be a new cataclysmic variable (U Gem-type, dwarf nova). Moreover, we know that this object is a cluster member (see Fig. 3). The star shows an outburst of about 3 mag and, though we did not observe the entire brightening, we would highlight that the magnitude was still increasing on the first night; thus we are able to say that the maximum brightness was reached immediately after.

We can estimate the orbital period, P_{orb} , and the recurrence time, T_n , from the decay time, $\tau_d = \Delta t / \Delta m$ [days mag $^{-1}$] and the amplitude, Δm (Warner, 1995, Eqs. (3.5), (3.1), respectively). Assuming for Δt and Δm the values 3.33 ± 0.50 d and 2.87 ± 0.31 mag respectively, we find $P_{\text{orb}} = 2.54 \pm 1.41$ h and $T_n = 13.9 \pm 10.6$ d. However, our light curve (Fig. 7) seems to rule out T_n values shorter than 8 d.

The variable B8 shows a large-amplitude light curve (Fig. 7) over a quite short 7 d time span. The cataclysmic nature of B8 has been confirmed spectroscopically by Kaluzny et al. (1997) who also notes that B8 exhibits red $V - I$ colour while in a low state.

Following the same procedure used for 06289_9 and assuming $\tau_d = 1.3 \pm 0.3$ d mag $^{-1}$ for B8, we find $P_{\text{orb}} = 2.97 \pm 1.63$ h and $T_n = 11.4 \pm 8.5$ d. The T_n value is compatible with the 7 d periodicity (Fig. 7). A membership probability is not available for B8. However, using the Eqs. (3.3) and (3.4) after

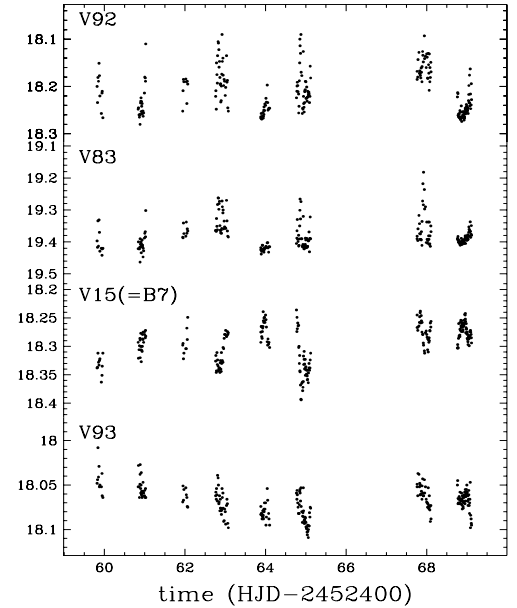


Fig. 6. Variable stars showing irregular fluctuations.

Warner (1995), we obtain $M_{V_{\text{min}}} = 8.06 \pm 0.68$ mag and $M_{V_{\text{max}}} = 4.97 \pm 0.42$ mag. In turn, these values give two estimates for the distance modulus of B8, i.e., 13.82 ± 0.68 mag and 14.20 ± 0.42 mag. We note that the first is in agreement with the distance modulus of the cluster. Kaluzny et al. (1997) assumed that B8 belongs to the cluster, finding $M_{V_{\text{max}}} = 5.2$ mag and $M_{V_{\text{min}}} = 7.6$, i.e., values very similar to ours. B8 is located at $4'$ from the center, and we can only conclude that the membership of this star is very probable.

4.4. Contact binaries

The simplest cases of eclipsing systems are the contact binaries (also named W UMa systems); they show short periods and continuous variability and therefore can be easily recognized and classified. We detected 29 of these variable stars; they have $P < 0.40$ days and very well defined light curves. The complete list and the light curves are reported in the Appendix. Table 4 lists the stars likely belonging to NGC 6791 (see above); their light curves are shown in Fig. 8. The very short periods and the secondary minima occurring at $\phi \approx 0.5$ indicate binaries with circular orbits, as is also the case for stars with small amplitudes (in 7 cases we have amplitudes less than 0.20 mag: V3, V4, V5, V8, V23, V40 and 01441_8). The average error bar on the period estimates is of the order of $4-5 \times 10^{-5}$ d.

However, we note that the stellar surfaces are not homogeneous since the maxima are often at different heights. Therefore, binarity and activity are probably combined here. In particular, the shape of the light curves of V4 (comparing RK96, M02 and our data) and V7 (comparing K93 and our data) have changed a lot; we suppose that stellar spots strongly modify the light curves. Proximity effects are also responsible for the large amplitudes observed for 01434_3 (Fig. 8, last panel) and 00766_5. We also found different periods for V118 (0.306321 d) and V124 (0.320143 d) compared to H05.

As for membership, the probabilities provided by Cudworth are 78%, 98% and 98% for V3, V4 and V5, respectively. Indeed, they are very close to the cluster center ($4'5$, $2'1$ and $2'8$, respectively).

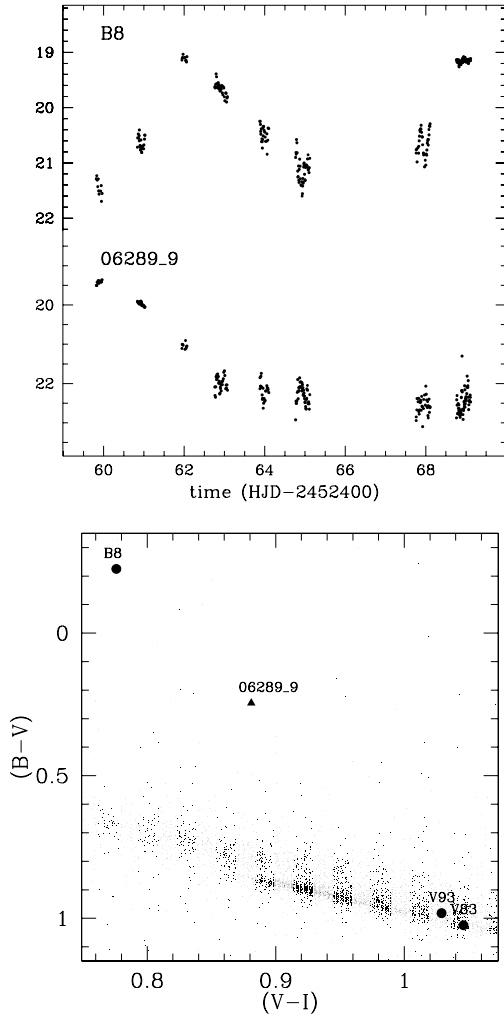


Fig. 7. *Top:* light curves of B8 (CV star) and 06289_9 (candidate CV). *Bottom:* positions in the two-colour diagram for two irregular stars (V83 and V93), for the cataclysmic variable B8 when in a low state, and for the new variable candidate 06289_9.

We suggest that 01441_8, V118, V8, V117 and V7 are also contact binaries belonging to NGC 6791. To further verify this hint, we calculated their distance by using the P - L - C relation given by Rucinski (2003); they turn out to have distance moduli (13.28, 13.28, 13.48, 13.28 and 13.18, respectively) very similar to that of the cluster (13.35).

Moreover, these stars are located at similar angular distances from the cluster center (6'2, 7'2, 7'1, 7'2 and 6'3, respectively). Figure 9 shows how the distance modulus of the cluster is in better agreement with those of the stars we proposed as cluster members than with those of the previously known members. Their positions in the CMDs (Fig. 10, filled circles) are similar to those of stars in the sample with $V < 7.5$ whose parallaxes have been determined by HIPPARCOS (Rucinski 2003). We also note that most of the cluster members are near the turnoff point.

4.5. Eclipsing variables

In the cases of detached or semi-detached eclipsing binaries the classification and membership tasks are different from the case of contact binaries. Table 5 lists the systems for which we could determine periods; their light curves are shown in Fig. 11. We

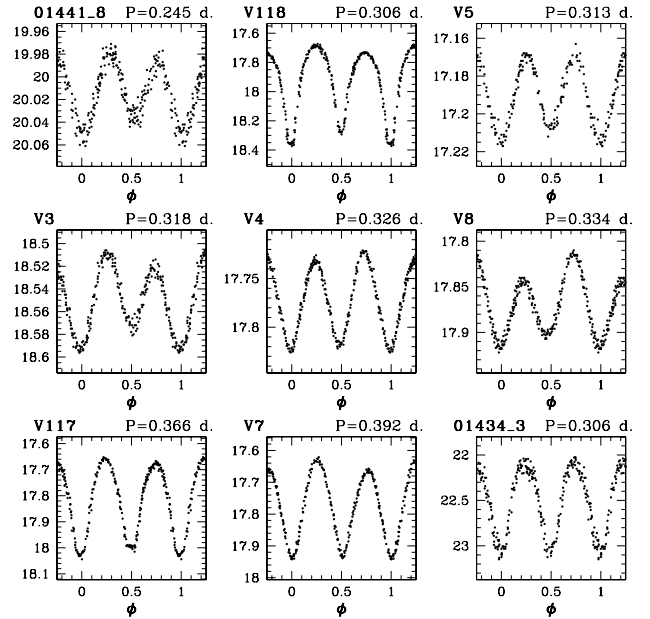


Fig. 8. The light curves of the contact binaries that are likely members of NGC 6791. The case of 01434_3 (amplitude much larger than 0.75 mag) is also shown in the last panel.

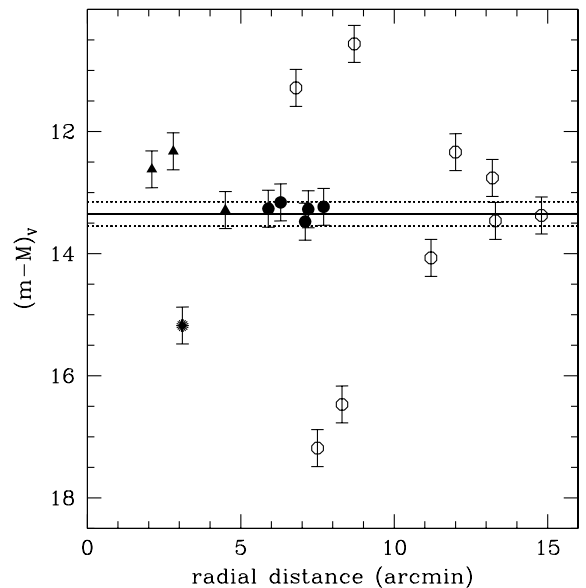
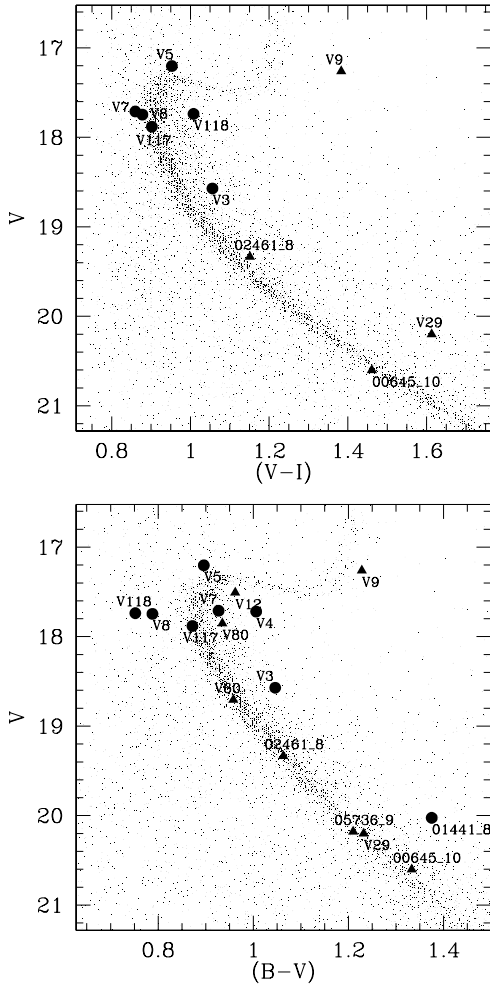


Fig. 9. The $m - M$ values calculated for contact binaries by means of the Rucinski (2003) P - L - C relation plotted against the distance from the cluster center. Triangles indicate the stars whose membership has been proposed by M03, the filled circles the stars whose membership has been proposed by us, and the open circles the stars that we suggest do not belong to NGC 6791. The starred point indicates the star 09891_9 which does not belong to the cluster on the basis of the proper motion (B06). The $(m - M)_V$ value for the cluster (solid line) with an error bar of ± 0.20 mag (dashed lines) is also shown.

still have short-period cases where we can reconstruct the complete light curve, as for the classical examples of β Lyr variables (V29, 01558_5 and 00331_3). V9 is a more complicated β Lyr system in which spots produce maxima with different heights. Indeed, it has been classified as an RS CVn variable by M05 and B03; they also observed a “shift of the modulation wave from 1995 to 2002.

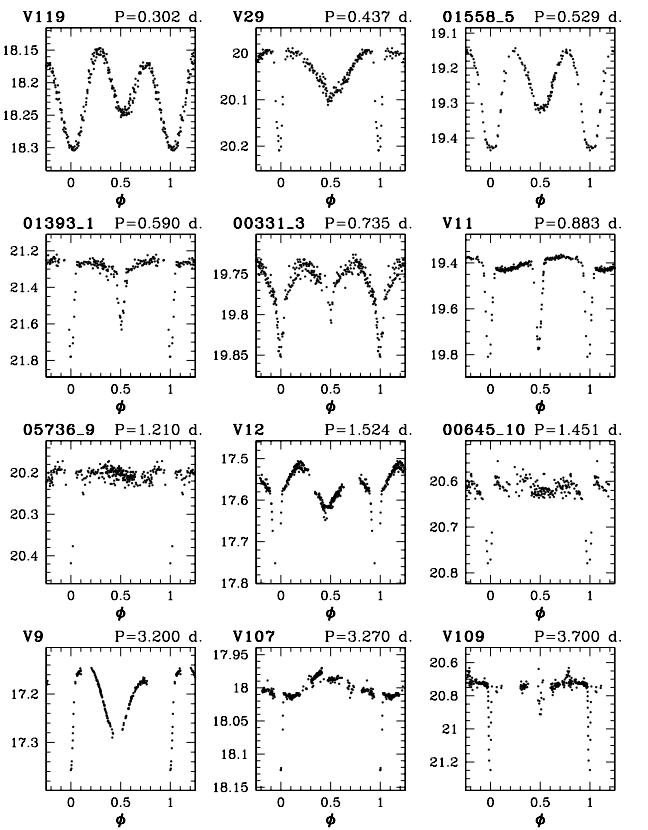
Table 4. Coordinates and light curve parameters of the contact binaries (W UMa systems, EW) belonging to NGC 6791. V is the brightness at maximum and T_0 is the time of the primary minimum.

Star	α_{2000}	δ_{2000}	V [mag]	$\langle B - V \rangle$ [mag]	$\langle V - I \rangle$ [mag]	Ref.	T_0 [HJD-2 452 400]	Period [d]	Ampl. [mag]	Notes
01441_8	19.339422	37.778118	19.98	1.38		k	63.073	0.24544	0.07	likely memb.
V118	19.347500	37.651222	17.68	0.75	1.01	s	59.912	0.30623	0.70	likely memb.
V5	19.346258	37.813354	17.19	0.90	0.95	k	60.221	0.31274	0.05	member (98%)
V3	19.354380	37.769349	18.51	1.05	1.06	k	59.798	0.31764	0.09	member (78%)
V4	19.348396	37.806652	17.72	1.01		k	59.591	0.32568	0.10	member (98%)
V8	19.341938	37.865810	17.81	0.79	0.88	k	59.896	0.33406	0.10	likely memb.
V117	19.343433	37.665848	17.66	0.87	0.90	k	59.987	0.36644	0.38	likely memb.
V7	19.340271	37.821892	17.63	0.93	0.86	k	59.820	0.39174	0.31	likely memb.

**Fig. 10.** The CMDs for the binary systems belonging to NGC 6791. Filled circles are contact binaries (W UMa stars), triangles are detached or semi-detached systems (β Per or β Lyr systems).

We note that our period for V119 is quite different from that given by H05 (0.1133 days); the new period makes this star an intermediate case between semi-detached and contact systems. Error bars on the periods in Table 5 are $\sim 10^{-4}$ d for $P < 1.0$ d, $\sim 10^{-3}$ d for $1.0 < P < 2.0$ d and a bit larger for $P > 3.0$ d.

Some variables show very sharp eclipses and out-of-eclipse variability due to different levels of stellar activity (05736_9, 00645_10, V109, 01393_1, V11 and V107; for the period of the latter star we prefer the longer of the two values given by M05).

**Fig. 11.** The light curves of short-period detached or semi-detached eclipsing binaries.

In many cases we observed one eclipse only and we cannot give any value for the period, unless it has been given in the previous studies, as for the cluster member V80 (86% on the basis of the Cudworth membership probability). We also note that the amplitude we observed in V80 is much larger than that reported by B03.

To establish the membership of these eclipsing systems is not an easy task, since binary effects should be taken into account when considering colors and magnitudes. However, on the basis of the distance from the cluster center and their position in the CMDs, we can argue that V60, 02461_8 (both single-event eclipsing binaries), 05736_9, V29 and 00645_10 are very probable members. This hint is corroborated by the membership probabilities for V60 and 02461_8, which are 91% and 88% respectively.

Table 5. Eclipsing variables with well defined light curves. EA stands for a β Per system, EB for a β Lyr one. V is the brightness at maximum and T_0 is the time of the primary minimum. Also B4, V60 and 02461_8, whose parameters are reported in the Appendix, are possible cluster members. The last column shows the Cudworth membership probability (when available).

Star	Type	α_{2000}	δ_{2000}	V	$\langle B - V \rangle$	$\langle V - I \rangle$	Ref.	T_0	Period	Ampl.	Notes
				[mag]	[mag]	[mag]		[HJD-2 452 400]	[d]	[mag]	
V119	EB	19.351961	37.916328	18.15	1.13	1.33	k	59.879	0.30197	0.15	member?
V29	EB	19.354796	37.751386	20.00	1.23	1.61	k	69.012	0.43662	0.22	likely memb.
01558_5	EB	19.372697	37.953469	19.15				69.028	0.52910	0.28	likely non-memb.
01393_1	EA	19.329588	37.970392	21.23				59.326	0.58998	0.56	likely non-memb.
00331_3	EB	19.352367	37.864391	19.73	1.20	1.36	k	68.815	0.7347	0.13	member?
V11	EA	19.342575	37.804802	19.38	0.96	1.22	k	67.875	0.8833	0.48	member?
05736_9	EA	19.348484	37.721855	20.20	1.21		k	68.333	1.210	0.29	likely memb.
V12	EB	19.345259	37.849083	17.52	0.96		k	64.103	1.524	0.06	member (96%)
00645_10	EA	19.354692	37.710104	20.60	1.33	1.46	k	60.893	1.451	0.20	likely memb.
V9	EB	19.346634	37.777035	17.15	1.23	1.38	k	63.873:	3.2	>0.2	member (82%)
V107	EA	19.355068	37.761553	17.97	0.93	1.00	k	64.433	3.27	0.24	member?
V109	EA	19.342716	37.793961	20.73	1.46	1.60	k	69.021	3.70	0.86	member?

The special cases of V9 and B4 deserve attention. V9 is the binary closest to the center and its membership probability is 82%. However, it looks a very evolved object in the CMD; its period (3.2 d) and activity (see above) are also more typical for a Main Sequence star. Therefore, its membership is very doubtful.

The Cudworth membership probability for B4 is only 40%, but in the CMDs B4 belongs to a little “clump” of very blue stars. This location is in agreement with the results of Liebert et al. (1994) and therefore B4 is likely a blue extended horizontal-branch star belonging to NGC 6791. The star is classified by M02 and M03 (who consider it a non-member) as an eclipsing binary, but we note that the light curve could also result from a rotational modulation.

Other possible members are: V107, 00331_3, V109 and V11, considering that they are within 6'4 radius from the cluster center. The location in the CMDs of the eclipsing binaries belonging to NGC 6791 is shown in Fig. 10 (triangles).

4.6. Rotational variables

We found 89 variables whose light curves are characterized by small amplitude (usually less than 0.10 mag) and continuous variability. It is difficult to ascribe such variability to contact binaries undergoing grazing eclipses, since they should be less numerous than those having partial eclipses, since grazing eclipses occur only for a particular orientation of the orbital plane. Our hypothesis is that in most cases this variability results from spots carried by the stellar rotation; under this hypothesis, a large variety of light curves can be produced. Of course, we cannot rule out that a small fraction of these light curves might be actually generated by grazing eclipses.

The complete list of the rotational variables and their light curves is given in the Appendix. Here we discuss some examples. If the inclination of the rotational axis causes the progressive disappearance of the largest spots, the light curve displays continuous variation, which could be sine shaped in the simplest cases (a fraction of the spots is always visible; it can also produce Cepheid-like variability, as in the 001606_1 case, Fig. 12), or with a standstill (the hot or cold spots totally disappear; 00513_2 in Fig. 12) or, more commonly, it can be distorted by other spots besides the largest ones (00471_12 in Fig. 12). In cases of very active stars, a secondary wave also occurs (01175_5 in Fig. 12). Since the second wave often covers less than half of the period, these rotational variables can be distinguished from eclipsing

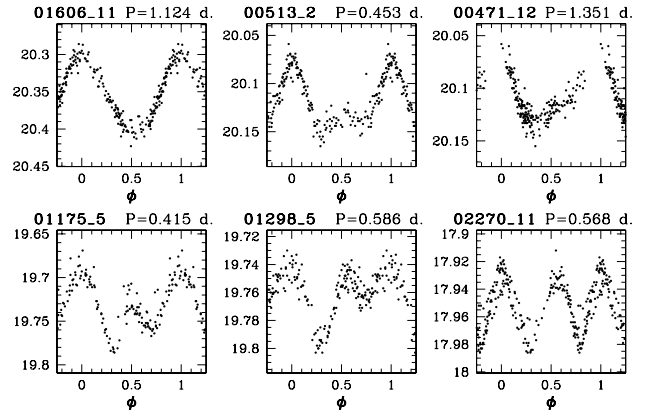


Fig. 12. The light curves of a small sample of rotational variables, illustrating the growing importance of the second wave.

binaries; we also note that the amplitude ratio between the first and second waves can be very different.

Also in the three cases in which the full amplitude is larger than 0.10 mag (V2, 02006_1 and 07483_9) rotational effects explain the observed features better than eclipses. For example, the light curves of V2 ($P = 0.273$ d) and 01298_5 ($P = 0.586$ d; see Fig. 12) show typical eclipsing binary behaviour, but the amplitudes, the periods, and, mainly, the asymmetries are more typical of a rotational effect. The case of 02270_11 is different (Fig. 12). Its light curve is very similar to that of a contact binary, but it does not repeat exactly, and unusual scatter is observed through the cycle. We also note that this non-repetitive behaviour of the light curves, due to the spot activity, is the reason why several variables stars show residual standard deviations higher than expected.

Our periods for V34, V37 and V38 are approximately half of those given by M02, since these authors classified these variables as ellipsoidal ones; the large amplitudes (0.18, 0.06 and 0.13 mag) are more in favour of a variability resulting from large spots, rather than the purely geometrical effect of tidally distorted stars. We also note that V37 did not show any flare activity similar to that reported by M02 during our survey. We have also revised the classification of V16, considered an eclipsing binary by M02 and M03.

Table 6. Rotational variables belonging to the cluster. V is the mean brightness value. T_0 indicates the time of the maximum brightness. The last column shows the membership probability (when available) or our photometric membership. The two uncertain cases (V41 and V14) are also listed (see text).

Star	Type	α_{2000}	δ_{2000}	V	$\langle B - V \rangle$	$\langle V - I \rangle$	Ref.	T_0	Period	Ampl.	Notes
				[mag]	[mag]	[mag]		[HJD-2 452 400]	[d]	[mag]	
04803_9	RO1	19.347698	37.796043	21.81	1.33	1.84	s	61.799	1.1034	0.17	member (B06)
V82	RO1	19.344366	37.793381	19.01	1.00	1.02	k	56.481	1.1568	0.04	likely memb.
06553_9	RO1	19.349134	37.672577	19.26	1.04	1.13	s	61.421	1.3485	0.08	likely memb.
01724_9	RO1	19.344957	37.785362	20.73	1.29	1.69	s	64.410	1.6130	0.17	likely memb.
V38	RO1	19.351021	37.768288	18.82	0.96		k	55.630	1.96	0.13	member (92%)
03079_9	RO1	19.346190	37.754753	19.23	1.14	1.26	k	66.630	2.640	0.07	member (93%)
V14	RO1	19.347687	37.756874	18.58	0.93	1.05	k	55.933	5.45	0.05	non-member (0%)
V48	RO1	19.352076	37.718506	17.51	0.88		k	65.223	5.65	0.09	member (96%)
V17	RO1	19.344135	37.817928	17.92	1.20	1.28	k	63.211	6.523	0.04	member (88%)
V51	RO1	19.353382	37.748795	19.94	1.22	1.21	k	63.624	6.72	0.09	likely memb.
V52	RO1	19.355795	37.771935	17.49	0.88	0.88	k	64.345	7.06	0.03	likely memb.
V53	RO1	19.350233	37.743187	18.72	0.89	0.93	k	69.294	7.47	0.04	member (86%)
00436_3	RO2	19.352205	37.878635	18.92	0.92	1.08	k	60.018	0.26601	0.04	likely memb.
07483_9	RO2	19.349997	37.746311	21.28	1.32	1.70	s	60.465	0.4375	0.17	likely memb.
V41	RO2	19.347492	37.806892	19.09				60.000	0.4798	0.07	member (77%)
V42	RO2	19.350058	37.714867	19.51	1.05	1.16	k	60.323	0.5068	0.10	member (92%)
V16	RO2	19.352108	37.802662	17.79	0.93	1.01	k	67.713	2.182	0.03	member (96%)

We count 33 rotational variables in the $10'$ -circle (i.e., $0.105 \text{ star/arcmin}^2$) centered on the cluster, while we have 56 variables in the remaining 924-arcmin^2 area (i.e., $0.061 \text{ star/arcmin}^2$). We have color indices ($B - V$ and/or $V - I$) for 48 stars; 33 of them have a radial distance less than $10'$ from the cluster center. We can confirm the membership for 6 stars having proper motion membership: V16, V38, V42, V48, V53 and 03079_9. We have no photometric indices for V41; however, it is at only $2'$ from the cluster center and its Cudworth probability membership is 77%. Therefore, we consider V41 a member. For V14 we have the opposite situation because this star is at $1'$ from the cluster center and its positions in the CMDs agree very well with a membership, but the proper motion measurements rule out that it can be a cluster member (0%) (see Fig. 13, V14 is displayed as a starred dot). As mentioned by M03, the positions of V17 in the CMDs are unusual. Other variables located below the subgiant branch like V17 were found in the open cluster M67 (Mathieu et al. 2003) and in the globular cluster 47 Tuc (Albrow et al. 2003). Probably these objects (named “red stragglers” or “sub-subgiant branch stars”) are the result of some kind of mass exchange between the members of a binary system.

Putting the rotational variables without proper motion measurements on the CMDs we could infer that 8 stars are located on or close to the MS (represented with filled circles in Fig. 13); thus we suggest that these 8 stars belong to the cluster as well. Among the variables at greater distances, for three stars (01149_2, 01122_4 and 00513_2, all located between $11'$ and $13'$) the membership is doubtful, since their position in the CMDs is unclear. The other stars show apparent magnitudes and/or color indices too discrepant to be considered active MS stars belonging to NGC 6791.

When considering the variables without color indices, only two (V41 and 01874_2) are at less than $10'$ from the cluster center. We know that V41 is a probable cluster member (membership probability 77%), but, at the moment, we have no valid reason to consider the other star as a member.

Table 6 lists the rotational variables we suggest as cluster members. The error bars on the period are $\sim 10^{-4}$ d for $P < 1.0$ d, $\sim 10^{-3}$ d for $1.0 < P < 2.0$ d, $\sim 10^{-2}$ d for $2.0 < P < 5.0$ d; periods longer than 5.0 d are tentative. Figure 13 shows the

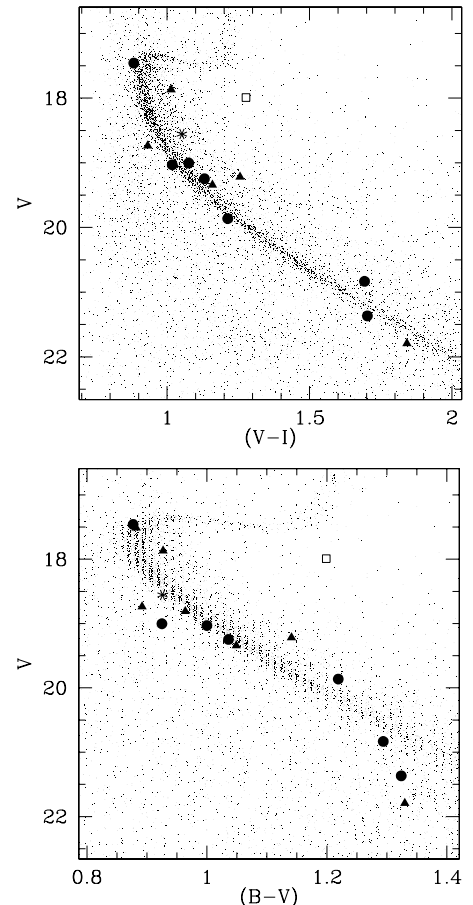


Fig. 13. $(V - I) - V$ and $(B - V) - V$ diagrams for NGC 6791. The rotational variables that we suggest may belong to the cluster are indicated with filled circles. *Triangles*: stars belonging to the cluster according to the Cudworth’s membership; *starred point*: V14, *open square*: V17 (see text for details about these stars).

CMDs with the rotational variables belonging to the cluster (Table 6) clearly indicated. We rejected as cluster members 16

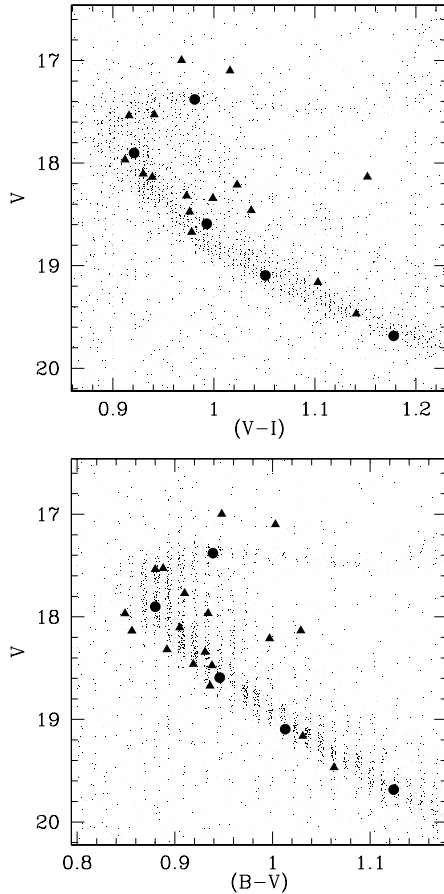


Fig. 14. $(B-V)-V$ and $(V-I)-V$ diagrams for NGC 6791. *Filled circles*: long-period variables that we suggest belong to the cluster. *Filled triangles*: long-period variables that belong to the cluster (membership probability higher than 76%).

stars out of 32 located within $10'$ from the cluster center; i.e., we considered them to be stars of the Galactic field. We note that the resulting density of the Galactic field ($0.051 \text{ star/arcmin}^2$) superimposed on the cluster is in good agreement with that of the surrounding galactic disk field ($0.061 \text{ star/arcmin}^2$, see above), especially considering that Poisson statistics supply uncertainties around ± 0.01 on the density values.

The stellar rotation and the activity level are both expected to be small for single stars as old as NGC 6791. Therefore we suggest that the rotational variables belonging to the cluster are likely short-period binaries, whose rotational velocity and activity level have been enhanced by the tidal synchronization.

4.7. Long-period variables

We detected numerous stars having different mean magnitudes on the different nights. Their behaviours are more diversified than those of the stars we considered as spurious on the basis of their close similarities. The resulting power spectra are dominated by terms at very low frequencies, corresponding to periods often much longer than 10 d. These periods cannot be evaluated in a precise way, being comparable or, more frequently, longer than our time baseline. Therefore, we can only argue that these stars are variables, either in a periodic or in an irregular way. Since we detected many spotted stars, it is quite obvious to think that most of these long-period variables are spotted stars having a rotational periods longer than 10 d. The mean amplitude of

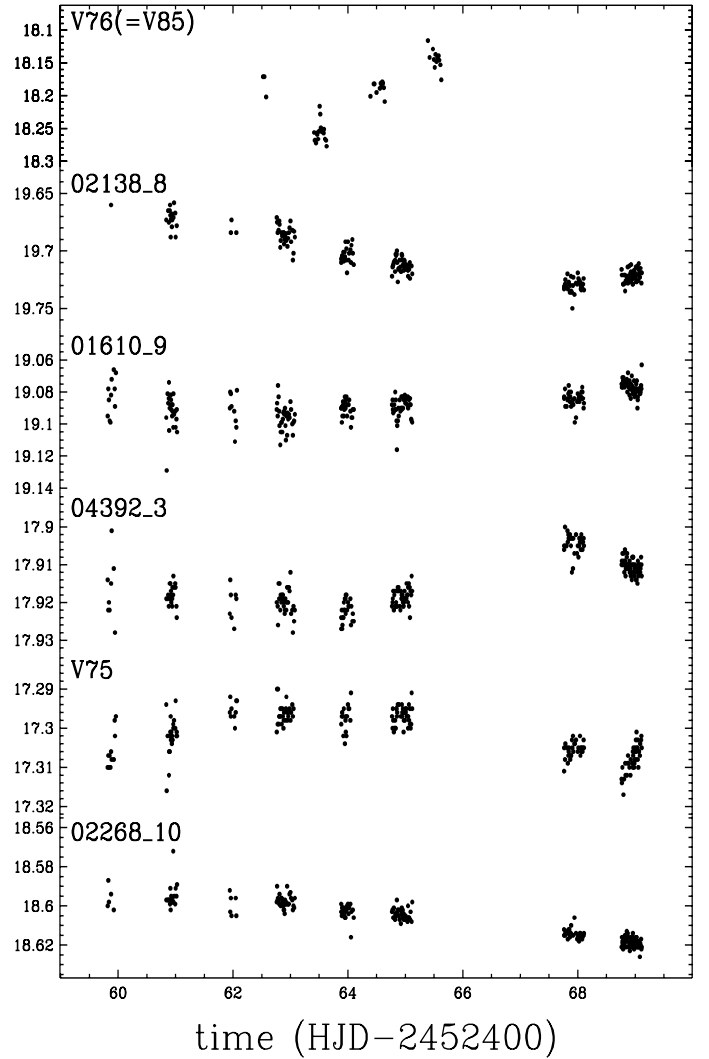


Fig. 15. Light curve of the suspect “red straggler” $V76 \equiv V85$ and the five stars that we suggest may belong to the cluster.

these stars is about 0.02 mag, except for 5 stars whose amplitude exceeds 0.1 mag.

Among the long-period variables, we used the Cudworth probabilities to establish the membership of 18 stars. In order to roughly estimate the membership of the remaining long-period variables we checked their locations in the CMDs, in the cases where at least one color is available. We suggest that 5 stars are likely members of NGC 6791: 02138_8, 01610_9, 04392_3, V75 and 02268_10 (see Fig. 14). They lie along the MS or the red-giant branch and, furthermore, they are all located at distances smaller than $8.5'$ from the cluster center. Looking at the position of the variable $V76 \equiv V85$ (memberships: 97%) in both CMDs, we suggest that this star could be similar to the “sub-subgiant branch” star V17. In Fig. 15 we show its light curve and those of the 5 stars that we suspect to belong to the cluster. Table 7 lists the long-period variables we suggest as cluster members; the entire sample is listed in the Appendix.

5. Conclusions

Our wide-field survey of NGC 6791 for the planetary-transit search allowed us to discover 260 new variable stars. When considering the membership probabilities given by Cudworth and B06, 13 of them belong to the cluster and one star (09831_9) is

Table 7. Long period variable stars that are likely members of NGC 6791 (ordered by increasing right ascension). Column 9 shows the membership probability (when available) or our photometric membership.

Star	α_{2000}	δ_{2000}	V [mag]	$\langle B - V \rangle$ [mag]	$\langle V - I \rangle$ [mag]	Ref.	Ampl. [mag]	Notes	Distance arcmin
02138_8	19.341864	37.749653	19.68	1.12	1.18	k	0.06	likely memb.	4.6
02444_8	19.342766	37.810604	18.34	0.93	1.00	k	0.02	member (78%)	4.4
00510_9	19.343704	37.796719	18.67	0.94	0.98	k	0.03	member (83%)	3.4
01610_9	19.344818	37.740486	19.09	1.01	1.05	k	0.02	likely memb.	3.0
V94	19.345139	37.743549	17.54	0.88	0.92	k	0.03	member (90%)	2.7
V95	19.345295	37.792412	19.16	1.03	1.10	k	0.07	member (93%)	2.3
V56(=V96)	19.345908	37.763525	17.01	0.95	0.97	k	0.04	member (98%)	1.6
04392_3	19.345982	37.870571	17.90	0.88	0.92	k	0.02	likely memb.	6.1
V75	19.346651	37.766308	17.38	0.94	0.98	s	0.01	likely memb.	1.0
04133_9	19.347109	37.777020	18.47	0.94	0.98	k	0.04	member (98%)	0.7
V76(=V85)	19.347192	37.764169	18.19	1.03	1.15	k	0.11	member (97%)	0.8
V86	19.347258	37.808815	19.44	1.06	1.14	k	0.03	member (83%)	2.3
V87	19.347996	37.749668	18.12	0.91	0.93	k	0.03	member (98%)	1.3
05740_9	19.348534	37.808022	17.96	0.93		k	0.03	member (95%)	2.2
06725_9	19.349329	37.724495	17.77	0.91		k	0.02	member (91%)	3.0
06796_9	19.349415	37.769268	18.46	0.92	1.04	k	0.03	member (92%)	1.0
V90	19.349686	37.746449	18.11	0.86	0.94	k	0.01	member (94%)	1.9
07680_9	19.350193	37.718224	18.32	0.89	0.97	k	0.03	member (98%)	3.5
V31	19.350683	37.785912	17.12	1.00	1.02	k	0.01	member (97%)	2.1
09376_9	19.351952	37.831886	18.21	1.00	1.02	k	0.01	member (92%)	4.6
09611_9	19.352139	37.773365	17.97	0.85	0.91	k	0.01	member (76%)	2.9
V58	19.354042	37.801240	17.52	0.89	0.94	k	0.05	member (87%)	4.6
02268_10	19.359475	37.731544	18.59	0.95	0.99	k	0.02	likely memb.	8.5

not member. On the basis of the distances from the cluster center and the positions in the CMDs, we suggest that another 11 stars are likely members, for 22 stars the membership is doubtful, and 137 stars are likely non-members. No photometric or kinematic data are available for 76 stars.

The variable star content of the cluster is very similar to that of the surrounding Galactic environment: in both samples we find rotational variables, contact and eclipsing systems. Contact binaries and rotational variables belonging to the cluster have the same characteristics as those located in the surrounding Galactic field. No evidence of pulsating variables has been found in NGC 6791, but this is not surprising, since it is a very evolved cluster and stars located in the instability strip or hotter pulsators have already left the MS.

The discovery of the new cataclysmic variable 06289_9 in addition to B8 and V15 adds another peculiarity to NGC 6791, making it unusual among the open clusters.

Acknowledgements. We are grateful to Kyle Cudworth kindly providing us with preliminary cluster membership probabilities. We also acknowledge Prof. Antonio Bianchini for his suggestions about the characteristics of the candidate cataclysmic variable and Giovanni Carraro for his useful comments. We thank the referee, Dr. J. Kaluzny, for his detailed report and useful comments. This work was funded by COFIN 2004 “From stars to planets: accretion, disk evolution and planet formation” by MIUR and by PRIN 2006 “From disk to planetary systems: understanding the origin and demographics of solar and extrasolar planetary systems” by INAF.

References

Albrow, M. D., Gilliland, R. L., Brown, T. M., et al. 2001, *ApJ*, 559, 1060
 Anthony-Twarog, B. J., Twarog, B. A., & Mayer, L. 2006, preprint
 [arXiv:astro-ph/0612549]
 Bedin, L. R., Salaris, M., Piotto, G., et al. 2005, *ApJ*, 624, 45

Bedin, L. R., Piotto, G., Carraro, G., King, I. R., & Anderson, J. 2006, *A&A*, 460, 27 (B06)
 Bruntt, H., Grundahl, F., Tingley, B., et al. 2003, *A&A*, 410, 323 (B03)
 Carpino, M., Milani, A., & Nobili, A. M. 1987, *A&A*, 181, 182
 Carraro, G., Villanova, S., Demarque, P., et al. 2006, *ApJ*, 643, 1151
 Chaboyer, B., Green, E. M., & Liebert, J. 1999, *AJ*, 117, 1360
 Ferraz-Mello, S. 1981, *AJ*, 86, 4
 Gratton, R., Bragaglia, A., Carretta, E., & Tosi, M. 2006, *ApJ*, 642, 462
 Hartman, J. D., Stanek, K. Z., Gaudi, B. S. et al. 2005, *AJ*, 130, 2241 (H05)
 Kaluzny, J. 2003, *Acta Astron.*, 53, 51 (K03)
 Kaluzny, J., & Rucinski, S. M. 1993, *MNRAS*, 265, 34 (KR93)
 Kaluzny, J., & Rucinski, S. M. 1995, *A&AS*, 114, 1
 Kaluzny, J., & Udalski, A. 1992, *Acta Astron.*, 42, 29
 Kaluzny, J., Stanek, K. Z., Garnavich, P. M., & Challis, P. 1997, *ApJ*, 491, 153
 King, I. R., Bedin, L. R., Piotto, G., Cassisi, S., & Anderson, J. 2005, *AJ*, 130, 626
 K6vacs, G., Zucker, S., & Mazeh, T. 2002, *A&A*, 391, 369
 Liebert, J., Saffer, R. A., & Green, E. M. 1994, *AJ*, 107, 1408
 Lomb, N. R. 1976, *Astrophysics and Space Science*, 39, 447
 Mathieu, R. D., van den Berg, M., Torres, G., et al. 2003, *AJ*, 125, 246
 McNamara, D. H. 2000, in *Delta Scuti and Related Stars* ed. M. Breger, & M. H. Montgomery, ASP Conf. Ser., 210, 373
 Mochejska, B. J., Stanek, K. Z., Sasselov, D. D., & Szentgyorgyi, A. H. 2002, *AJ*, 123, 3460 (M02)
 Mochejska, B. J., Stanek, K. Z., & Kaluzny, J. 2003, *AJ*, 125, 3175 (M03)
 Mochejska, B. J., Stanek, K. Z., Szentgyorgyi, A. H., et al. 2005, *AJ*, 129, 2856 (M05)
 Montalto, M., Piotto, G., Desidera, S., et al. 2007, *A&A*, 470, 1137
 Poretti, E. 2001, *A&A*, 371, 986
 Rucinski, S. M. 1995, *PASP*, 107, 648
 Rucinski, S. M. 2003, *New Astron. Rev.*, 48, 703
 Rucinski, S. M., Kaluzny, J., & Hilditch, R. W. 1996, *MNRAS*, 282, 705 (RK96)
 Stellingwerf, R. F. 1978, *ApJ*, 224, 953
 Stetson, P. B., Bruntt, H., & Grundahl, F. 2003, *PASP*, 115, 413
 Tammann, G. A., Sandage, A., & Reindl, B. 2003, *A&A*, 404, 423
 Vanicek, P. 1971, *Astrophysics and Space Science*, 12, 10
 Warner, B. 1995, *Cataclysmic Variable Stars* (Cambridge: Cambridge Univ. Press)

Online Material

Appendix A: List of identified variables

This Appendix includes the full list of the identified variables, separated according to our classification:

1. Pulsating, irregular and cataclysmic variables: Table A.1.
2. EW-type stars: Table A.2, Fig. A.1.
3. EA/EB-type stars: Table A.3.
4. Single-wave rotational variables: Table A.4, Figs. A.2, A.3.
5. Double-wave rotational variables: Table A.5, Fig. A.4.
6. Long-period variables: Table A.6.

Into the tables, for each star we give the name (a five-digit number followed by the chip number which the star belongs), coordinates, photometric data (always the V mag, $B - V$ color when available), informations about the variability (T_0 , period, amplitude), distance from the center (in arcmin) and finally the numerical value of the Cudworth's membership probability (reported in the column "Memb.").

In most cases, when membership probabilities were not available, in the same column the label "m" means that we retain the star belonging to the cluster, while "m?" and "nm" mean "uncertain membership" and "likely non-member" respectively. The label "nd1" means that no photometric data are available to advance hypothesis about the membership, but the star is located nearer than $10'$ from the center of the cluster. Finally "nd2" means that no photometric data are available and the star is located further than $10'$ from the center; in this case we strongly suggest that the star does not belong to the cluster.

Table A.1. Pulsating, irregular and cataclysmic variables. V is the minimum brightness for CVs and irregular, the mean brightness for pulsating variables. T_0 is the time of maximum brightness for pulsating stars.

Star	Type	α_{2000}	δ_{2000}	V [mag]	$\langle B - V \rangle$ [mag]	$\langle V - I \rangle$ [mag]	Ref.	T_0 [HJD-2 452 400]	Period [d]	Ampl. [mag]	Memb.	Distance [arcmin]
V123	HADS	19.362064	37.666034	17.08	0.45		k	59.559	0.06026	0.14	nm	11.8
01497_12	HADS	19.379083	37.812419	16.06				59.528	0.07227	0.40	nd2	22.2
00311_7	SXPhe	19.324628	37.716768	23.17				59.605	0.10443	0.10	nd2	17.0
00224_10	SXPhe	19.353639	37.710163	21.72	0.71	1.06	s	59.801	0.12261	0.20	nm	5.4
03653_3	RRc	19.347147	37.992413	17.21	0.57	0.58	k	59.937	0.32654	0.39	nm	13.3
00345_1	RRab	19.325082	37.964170	18.28				60.151	0.57866	0.72	nd2	20.0
V92	IRR	19.350754	37.766876	18.10	0.91		k			0.10	m	1.9
V83	IRR	19.346220	37.737232	19.10	1.02	1.05	k			0.07	m	2.4
V93	IRR	19.351452	37.785687	18.12	0.98	1.03	s			0.04	m	2.6
V15(=B7)	CV	19.352057	37.799019	18.26	0.20		k			0.06	98	3.3
B8	CV	19.343262	37.747833	20.64	-0.23	0.78	k			2.27	m	3.7
06289_9	CV	19.348976	37.770355	22.80	0.25	0.88	s			3.10	m (B06)	0.7

Table A.2. Contact binaries; V is the brightness at maximum and T_0 is the time of the primary minimum.

Star	α_{2000}	δ_{2000}	V [mag]	$\langle B - V \rangle$ [mag]	$\langle V - I \rangle$ [mag]	Ref.	T_0 [HJD-2 452 400]	Period [d]	Ampl. [mag]	Memb.	Distance [arcmin]
V122	19.360729	37.641436	20.92				59.614	0.22883	0.58	nd2	11.9
V115	19.330646	37.975902	20.70				59.473	0.23636	0.24	nd2	17.4
01407_8	19.339256	37.701576	21.52	0.64	1.25	k	59.447	0.24155	0.82	nm	7.5
01150_4	19.357227	37.962177	18.58	1.07	0.93	k	59.455	0.24510	0.27	nm	13.2
01441_8	19.339422	37.778118	19.98	1.38		k	63.073	0.24544	0.07	m	6.2
00144_2	19.334044	38.030701	19.19				59.457	0.24780	0.77	nd2	18.5
01670_10	19.357625	37.681442	16.64	1.14	1.24	k	59.729	0.25807	0.49	nm	8.7
V121	19.358063	37.932346	17.24	0.81	0.84	k	59.619	0.26742	0.71	nm	12.0
02291_11	19.371624	37.795464	19.15				59.582	0.26774	0.29	nd2	16.8
V23	19.338614	37.787781	16.92	1.04	1.23	k	59.915	0.27180	0.07	nm	6.8
V25	19.328426	37.713237	18.50				59.772	0.27730	0.56	nd2	14.4
00665_12	19.375697	37.713244	18.89				59.472	0.28369	0.41	nd2	20.0
09831_9	19.352356	37.780907	20.55	1.09	1.19	s	59.662	0.29488	0.3	nm (B06)	3.1
01434_3	19.350643	37.985512	22.10				59.831	0.30581	0.97	nd2	13.0
V118	19.347500	37.651222	17.68	0.75	1.01	s	59.912	0.30623	0.70	m	7.2
00721_11	19.365737	37.713858	15.53				59.491	0.31008	0.26	nd2	13.1
01701_2	19.341944	38.017998	18.72				59.534	0.31201	0.51	nd2	15.4
V5	19.346258	37.813354	17.19	0.90	0.95	k	60.221	0.31274	0.05	98	2.8
V3	19.354380	37.769349	18.51	1.05	1.06	k	59.798	0.31764	0.09	78	4.5
02030_4	19.353487	38.009422	19.04	1.19	1.42	k	59.614	0.31797	0.33	nm	14.8
V124	19.365150	37.681544	17.62	0.70	1.07	k	59.855	0.32014	0.58	nm	13.3
00766_5	19.367585	37.943904	22.31				59.466	0.32363	0.78	nd2	17.3
V4	19.348396	37.806652	17.72	1.01		k	59.591	0.32568	0.10	98	2.1
V27	19.336275	37.648720	18.47	0.82	1.29	k	59.763	0.33170	0.84	nm	11.2
V8	19.341938	37.865810	17.81	0.79	0.88	k	59.896	0.33406	0.10	m	7.1
V101	19.351563	37.640388	19.94	0.56		k	59.798	0.33480	0.29	nm	8.3
V117	19.343433	37.665848	17.66	0.87	0.90	k	59.987	0.36644	0.38	m	7.2
V7	19.340271	37.821892	17.63	0.93	0.86	k	59.820	0.39174	0.31	m	6.3
V40	19.327495	37.616839	19.67				60.101	0.39750	0.16	nd2	17.3

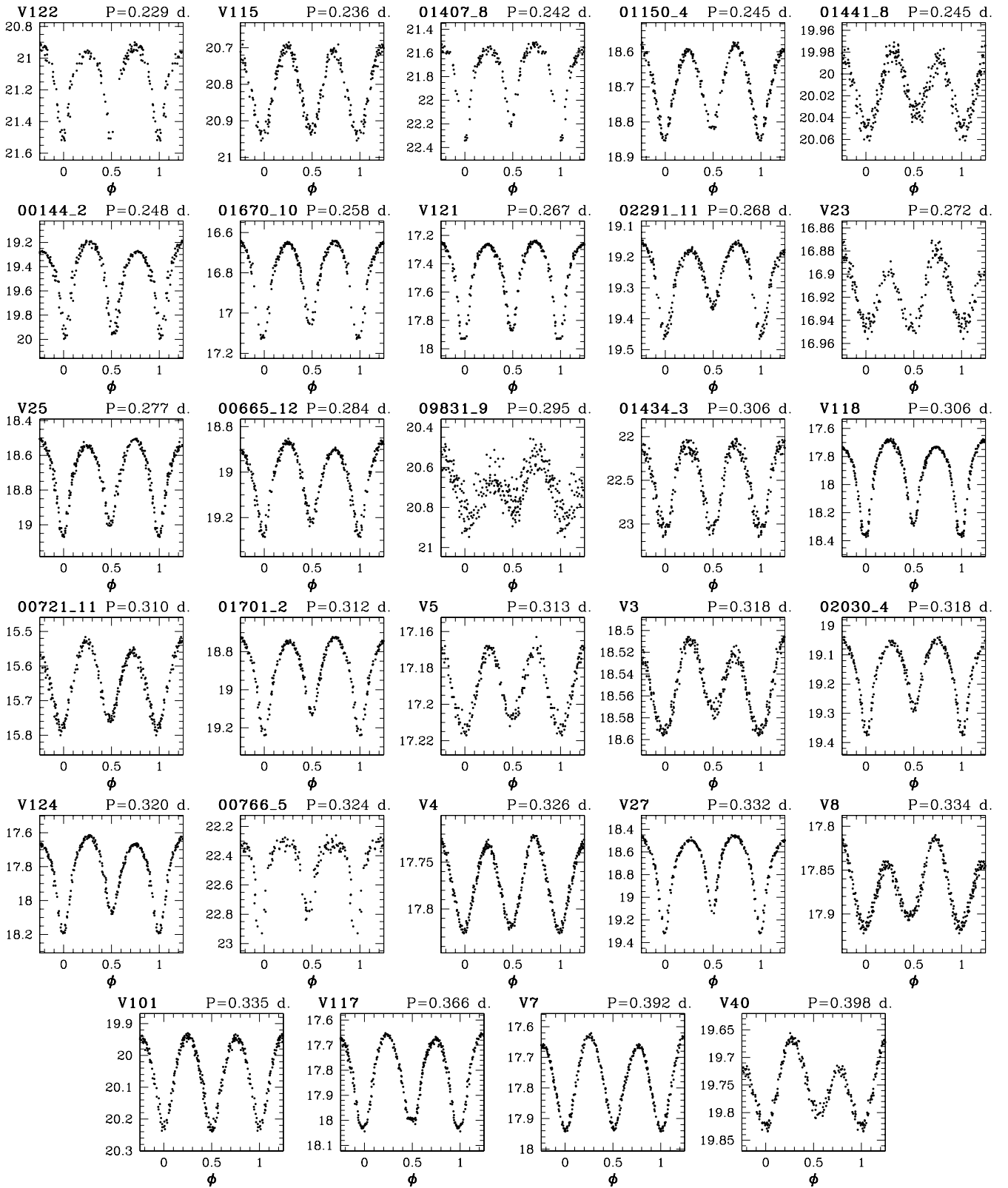


Fig. A.1. Contact variables.

Table A.3. Eclipsing variables. V is the brightness at maximum and T_0 is the time of the primary minimum.

Star	Type	α_{2000}	δ_{2000}	V [mag]	$\langle B - V \rangle$ [mag]	$\langle V - I \rangle$ [mag]	Ref.	T_0 [HJD-2 452 400]	Period [d]	Ampl. [mag]	Memb.	Distance [arcmin]	Notes
V119	EB	19.351961	37.916328	18.15	1.13	1.33	k	59.879	0.30197	0.15	m?	9.1	
B4	E:	19.353589	37.764290	17.87	-0.13	-0.15	k	54.788	0.39841	0.02	40	4.0	
V29	EB	19.354796	37.751386	20.00	1.23	1.61	k	69.012	0.43662	0.22	m	4.9	Light curve distortion at maximum light
01558_5	EB	19.372697	37.953469	19.15				69.028	0.52910	0.28	nd2	20.6	
01393_1	EA	19.329588	37.970392	21.23				59.326	0.58998	0.56	nd2	17.7	
00331_3	EB	19.352367	37.864391	19.73	1.20	1.36	k	68.815	0.7347	0.13	m?	6.4	
V11	EA	19.342575	37.804802	19.38	0.96	1.22	k	67.875	0.8833	0.48	m?	4.4	
05736_9	EA	19.348484	37.721855	20.20	1.21		k	68.333	1.210	0.29	m	3.0	
V12	EB	19.345259	37.849083	17.52	0.96		k	64.103	1.524	0.06	96	5.1	
00645_10	EA	19.354692	37.710104	20.60	1.33	1.46	k	60.893	1.451	0.20	m	6.0	
V9	EB	19.346634	37.777035	17.15	1.23	1.38	k	63.873	3.2	0.20	82	1.1	
V107	EA	19.355068	37.761553	17.97	0.93	1.00	k	64.433	3.27	0.24	m?	5.0	Minima at the very beginning of the night.
V109	EA	19.342716	37.793961	20.73	1.46	1.60	k	69.021	3.70	0.86	m?	4.0	
00219_11	EA	19.364048	37.827507	17.94	0.92	0.87	k	67.913		0.52	nm	11.9	
00663_4	EA	19.359652	37.894062	17.49	0.79	0.83	k	65.003		0.49	nm	11.0	
00671_2	EA	19.336983	37.903919	18.46	0.70	0.91	k	64.968		0.07	nm	11.2	
00828_5	EA	19.367917	37.885330	21.28				64.979		0.38	nd2	15.7	
00938_2	EA	19.338285	37.861633	20.57	1.20	1.80	k	67.867		0.60	nm	8.8	
00997_10	EA	19.355692	37.799655	19.58	0.76	0.83	k	68.020		0.20	nm	5.7	
01709_1	EA	19.330890	37.932268	18.04				64.818		0.32	nd2	15.5	
01731_10	EA	19.357813	37.672819	19.27	0.67	0.80	k	64.783		0.34	nm	9.1	Minimum at the very beginning of the night.
01780_8	EA	19.340677	37.655354	22.19		2.25	k	68.969		0.66	nm	8.7	
02461_8	EA	19.342779	37.741798	19.34	1.06	1.15	k	60.968		0.11	88	4.2	
01740_7	EA	19.330623	37.638774	21.30				69.007		0.33	nd2	14.8	Maybe another minimum at 64.40
02045_12	EA	19.381420	37.712211	17.16				68.030		0.26	nd2	24.0	Other minimum at 63.39
02241_11	EA	19.371472	37.827819	19.21				68.823		0.53	nd2	17.0	Maybe another minimum at 63.50
00346_5	EA	19.365356	37.929481	20.16				65.014		0.17	nd2	15.5	Other minimum at at 68.410. Short in time.
00631_12	EA	19.375473	37.649140	17.92				68.753		0.30	nd2	20.9	Minimum at the very beginning of the night.
01511_10	EA	19.357145	37.689907	19.74	1.45	1.86	k			0.50	nm	8.1	Two Minima at night extrema.
V60	EA	19.350189	37.762493	18.68	0.96		k	67.951		0.39	91	1.6	
V80	EA	19.351799	37.791061	17.90	0.94		k	67.607	4.631	0.10	86	2.9	Shallow eclipse ?
V108	EA	19.352606	37.823467	21.15	1.27	1.90	k	69.080		0.86	nm	4.5	

Table A.4. Rotational variables with a single-wave light curve. V is the mean brightness value. T_0 indicates the time of the maximum brightness.

Star	α_{2000}	δ_{2000}	V [mag]	$\langle B - V \rangle$ [mag]	$\langle V - I \rangle$ [mag]	Ref.	T_0 [HJD-2452 400]	Period [d]	Ampl. [mag]	Memb.	Distance [arcmin]
02268_12	19.382495	37.798839	17.42				60.323	0.30910	0.02	nd2	24.6
02418_3	19.349085	38.016541	21.68				59.901	0.36498	0.12	nd2	14.7
00513_2	19.336012	37.940765	20.12	1.18	1.51	k	60.786	0.45272	0.08	m?	13.3
02292_10	19.359535	37.710207	16.24	1.11	1.25	k	61.298	0.46371	0.06	nm	9.0
01497_11	19.368601	37.770512	18.58				61.737	0.56508	0.01	nd2	14.6
01776_4	19.354509	37.935883	19.70	0.99	1.16	k	61.154	0.68029	0.06	nm	10.9
00301_5	19.365041	37.906284	22.10				62.833	0.70170	0.21	nd2	14.5
00088_8	19.333437	37.744888	21.92				65.464	0.70594	0.11	nd2	10.5
V43	19.344337	37.641777	19.58	1.62	2.97	k	55.976	0.75759	0.08	nm	8.2
00554_8	19.335732	37.664570	21.32	1.22	1.48	k	65.543	0.821	0.13	nm	10.9
00612_10	19.354604	37.729215	22.97	0.79	2.42	s	68.050	0.91581	0.24	m?	5.3
01105_12	19.377359	37.737573	19.31				62.539	0.91746	0.04	nd2	21.0
00913_5	19.368442	37.859339	20.89				62.405	1.06386	0.24	nd2	15.4
04803_9	19.347698	37.796043	21.81	1.33	1.84	s	61.799	1.1034	0.17	m (B06)	1.5
01606_11	19.368978	37.736585	20.36				62.390	1.12360	0.10	nd2	15.0
V82	19.344366	37.793381	19.01	1.00	1.02	k	56.481	1.1568	0.04	m	2.9
V34	19.335878	37.736183	19.30	1.16	1.41	k	54.955	1.20486	0.18	nm	8.9
05302_3	19.344669	37.968491	18.90				63.224	1.3334	0.15	nd2	12.1
06553_9	19.349134	37.672577	19.26	1.04	1.13	s	61.421	1.3485	0.08	m	6.0
00471_12	19.374883	37.674950	19.35				61.900	1.3513	0.06	nd2	20.0
00110_5	19.363887	38.001389	21.69				62.103	1.4085	0.08	nd2	17.8
01874_2	19.342730	37.912987	21.96				64.944	1.5503	0.14	nd1	9.3
V111	19.346970	37.812141	20.67	1.46	1.66	s	61.673	1.5626	0.15	nm	2.5
V37	19.355072	37.852001	19.58	1.65	2.48	k	55.721	1.6130	0.06	nm	6.9
01724_9	19.344957	37.785362	20.73	1.29	1.69	s	64.410	1.6130	0.17	m	2.4
02285_10	19.359424	37.607155	19.26	1.34	1.57	k	63.495	1.6668	0.08	nm	12.8
01189_11	19.367513	37.809413	20.46				64.500	1.7242	0.10	nd2	14.0
00016_5	19.363396	37.997513	18.68	1.54	2.52	k	63.157	1.7858	0.07	nm	17.4
00732_12	19.375889	37.717569	19.39				61.992	1.852	0.04	nd2	20.1
00771_11	19.365949	37.766208	19.52				62.492	1.852	0.09	nd2	12.7
00676_1	19.326459	37.929277	20.54				65.481	1.887	0.11	nd2	18.0
V38	19.351021	37.768288	18.82	0.96		k	55.630	1.96	0.13	92	2.1
02103_7	19.332028	37.696796	19.57	1.65		k	60.891	2.041	0.05	nm	12.3
00575_12	19.375449	37.792459	19.63				65.359	2.214	0.02	nd2	19.5
01914_1	19.331830	37.878855	17.71	0.73		k	62.358	2.222	0.03	nm	13.2
03838_3	19.346848	37.964615	19.45	0.91	1.05	k	64.159	2.261	0.04	nm	11.6
V44	19.326970	37.694771	18.38				58.310	2.285	0.02	nd2	15.7
00321_1	19.324957	37.905996	19.49				65.394	2.326	0.04	nd2	18.3
00810_5	19.367793	37.865903	18.17				67.424	2.564	0.05	nd2	15.1
03079_9	19.346190	37.754753	19.23	1.14	1.26	k	66.630	2.640	0.07	93	1.7
01821_12	19.380347	37.604033	20.13				70.829	2.647	0.06	nd2	25.1
01309_11	19.367871	37.748052	20.81				61.125	2.692	0.05	nd2	14.2
01956_12	19.380972	37.626492	21.39				63.833	2.699	0.06	nd2	25.0
00815_1	19.327108	37.861623	19.75				63.358	2.836	0.05	nd2	15.8
01659_8	19.340244	37.694355	21.27	1.51	1.85	k	64.446	2.840	0.17	nm	7.2
00293_11	19.364252	37.703417	15.82	0.80	0.88	k	63.606	2.941	0.05	nm	12.2
00215_5	19.364447	37.898928	22.26				65.340	3.15	0.14	nd2	13.9
03209_10	19.362653	37.732028	18.61	1.54	2.57	k	66.016	3.17	0.06	nm	10.7
01313_1	19.329261	38.025661	21.27				62.466	3.704	0.10	nd2	20.3
00277_8	19.334366	37.776566	19.52	1.54	2.68	k	60.691	4.167	0.05	nm	9.7
00179_5	19.364283	38.002234	17.18	0.91	0.90	k	64.764	4.323	0.04	nm	18.0
03039_10	19.362130	37.815850	16.58	0.79	0.87	k	65.634	4.423	0.02	nm	10.4
01555_4	19.355373	37.961205	21.22				69.673	4.546	0.09	nd2	12.5
02614_11	19.372592	37.625244	17.22				70.152	4.763	0.04	nd2	19.6
01149_2	19.339287	37.966995	17.80	0.90	0.93	k	67.803	5.0	0.04	m?	13.3
02815_3	19.348427	37.967987	19.87	1.68	2.40	k	60.828	5.0	0.05	nm	11.8
V46	19.355272	37.798869	18.65	1.18	1.36	k	56.886	5.2	0.14	nm	5.4
00357_5	19.365449	37.996214	20.91				63.108	5.3	0.07	nd2	18.3
01484_7	19.329583	37.791249	20.30	1.63		k	67.924	5.3	0.03	nm	13.2
V14	19.347687	37.756874	18.58	0.93	1.05	k	55.933	5.45	0.05	0	0.9
V48	19.352076	37.718506	17.51	0.88		k	65.223	5.65	0.09	96	4.3

Table A.4. continued: other rotational variables with a single-wave light curve. V is the mean brightness value. T_0 indicates (one of) the times of maximum brightness.

Star	α_{2000}	δ_{2000}	V [mag]	$\langle B - V \rangle$ [mag]	$\langle V - I \rangle$ [mag]	Ref.	T_0 [HJD-2 452 400]	Period [d]	Ampl. [mag]	Memb.	Distance [arcmin]
00615_7	19.325908	37.753712	20.59				59.885	5.882	0.14	nd2	15.8
V89	19.349068	37.776783	18.75	0.88	1.20	s	63.447	5.884	0.05	nm	0.8
00188_12	19.373720	37.632076	21.78				67.253	6.25	0.06	nd2	20.1
V17	19.344135	37.817928	17.92	1.20	1.28	k	63.211	6.523	0.04	88	3.9
01122_4	19.357346	37.914520	18.84	1.03	1.12	k	65.843	6.69	0.11	m?	10.8
03056_3	19.347979	37.869431	17.10	0.89	0.97	k	66.673	6.70	0.07	nm	5.9
V51	19.353382	37.748795	19.94	1.22	1.21	k	63.624	6.72	0.09	m	4.0
00640_10	19.354585	37.604724	17.97	0.68	0.77	k	66.173	6.8	0.03	nm	11.0
V52	19.355795	37.771935	17.49	0.88	0.88	k	64.345	7.06	0.03	m	5.5
V53	19.350233	37.743187	18.72	0.89	0.93	k	69.294	7.47	0.04	86	2.3
01431_10	19.357001	37.763810	17.72	1.33	1.45	k	67.953	7.64	0.26	nm	6.4
01616_11	19.369060	37.767818	17.26				69.157	7.70	0.05	nd2	14.9
01478_3	19.350523	37.862484	17.15	1.03	1.11	k	72.123	7.96	0.07	nm	5.7
05877_9	19.348616	37.767616	20.22	1.32	1.49	k	64.272	8.0	0.12	nm	0.5

Table A.5. Rotational variables with a double-wave light curve. V is the mean brightness value. T_0 indicates (one of) the times of maximum brightness.

Star	α_{2000}	δ_{2000}	V [mag]	$\langle B - V \rangle$ [mag]	$\langle V - I \rangle$ [mag]	Ref.	T_0 [HJD-2 452 400]	Period [d]	Ampl. [mag]	Memb.	Distance [arcmin]
00436_3	19.352205	37.878635	18.92	0.92	1.08	k	60.018	0.26601	0.04	m	7.1
V2	19.354875	37.766689	19.74	0.93	1.21	k	59.712	0.27344	0.17	nm	4.9
02006_1	19.332258	38.043080	21.54				60.448	0.37500	0.19	nd2	19.8
01175_5	19.370209	37.998342	19.73				59.918	0.41481	0.09	nd2	20.8
00536_11	19.365067	37.716529	19.13				60.460	0.43740	0.03	nd2	12.6
07483_9	19.349997	37.746311	21.28	1.32	1.70	s	60.465	0.4375	0.17	m	2.1
V41	19.347492	37.806892	19.09				60.000	0.4798	0.07	77	2.2
V42	19.350058	37.714867	19.51	1.05	1.16	k	60.323	0.5068	0.10	92	3.7
01362_7	19.329000	37.662097	20.53				60.502	0.5560	0.08	nd2	15.1
02270_11	19.371548	37.794338	17.95				60.525	0.5679	0.05	nd2	16.8
01298_5	19.371044	38.002255	19.76				60.402	0.5859	0.06	nd2	21.4
V16	19.352108	37.802662	17.79	0.93	1.01	k	67.713	2.182	0.03	96	3.4
00568_2	19.336329	37.881542	18.52				60.007	2.704	0.08	nd2	10.6
00019_7	19.323382	37.710172	18.95				65.473	5.882	0.12	nd2	17.9

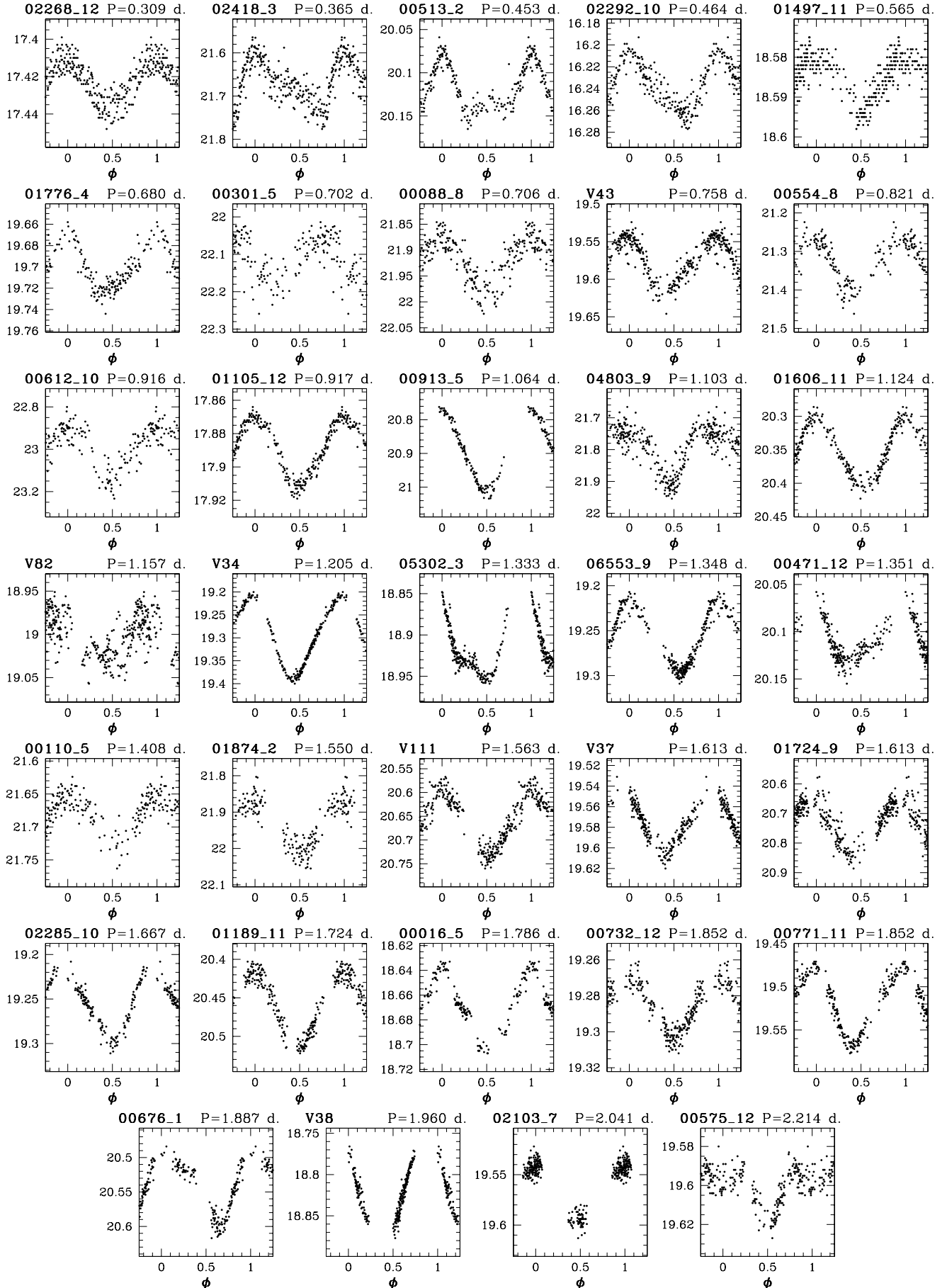


Fig. A.2. Rotational variables with a single-wave light curve, in some cases very distorted.

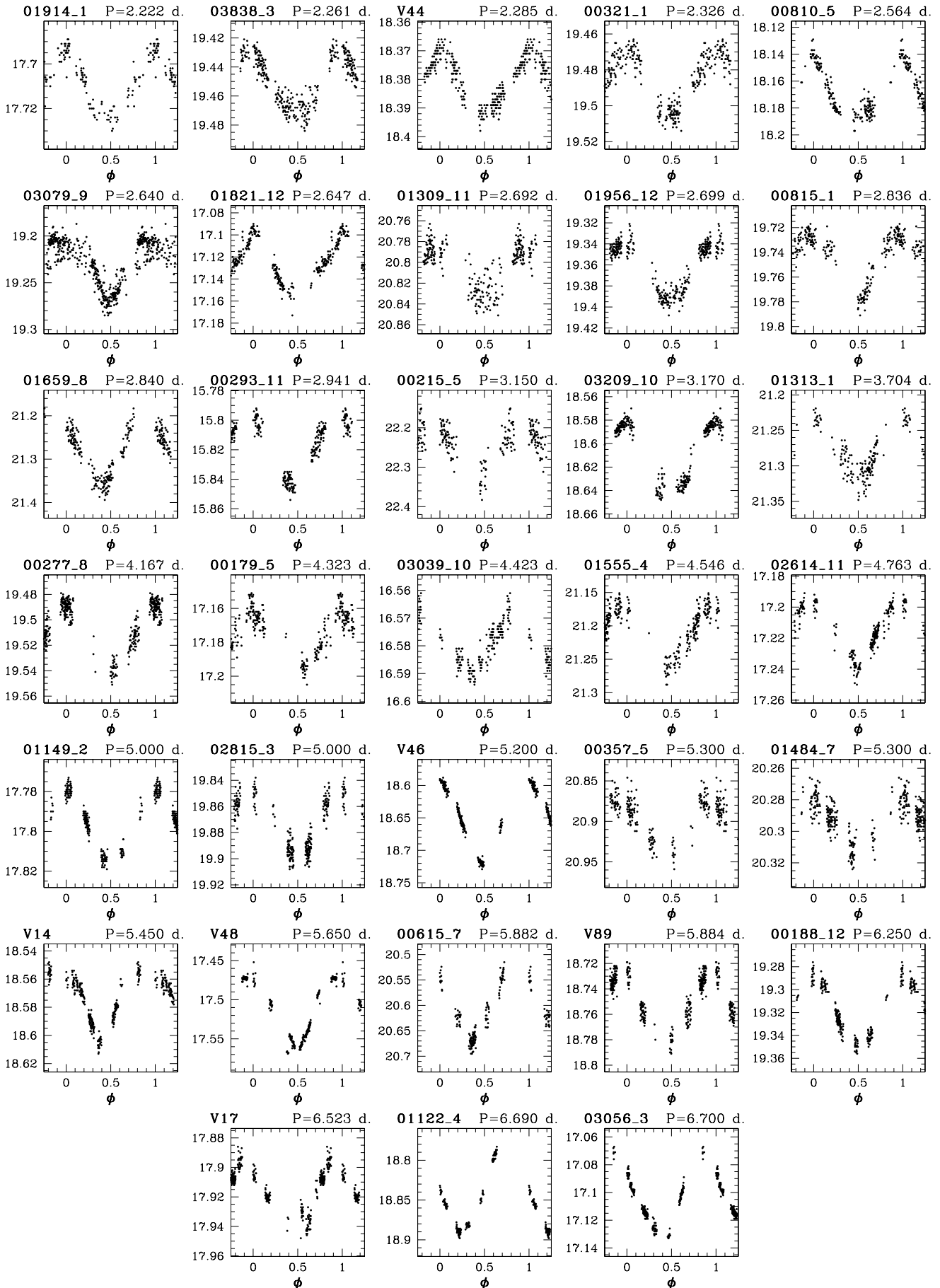


Fig. A.3. Rotational variables with a single-wave light curve, in some cases very distorted.

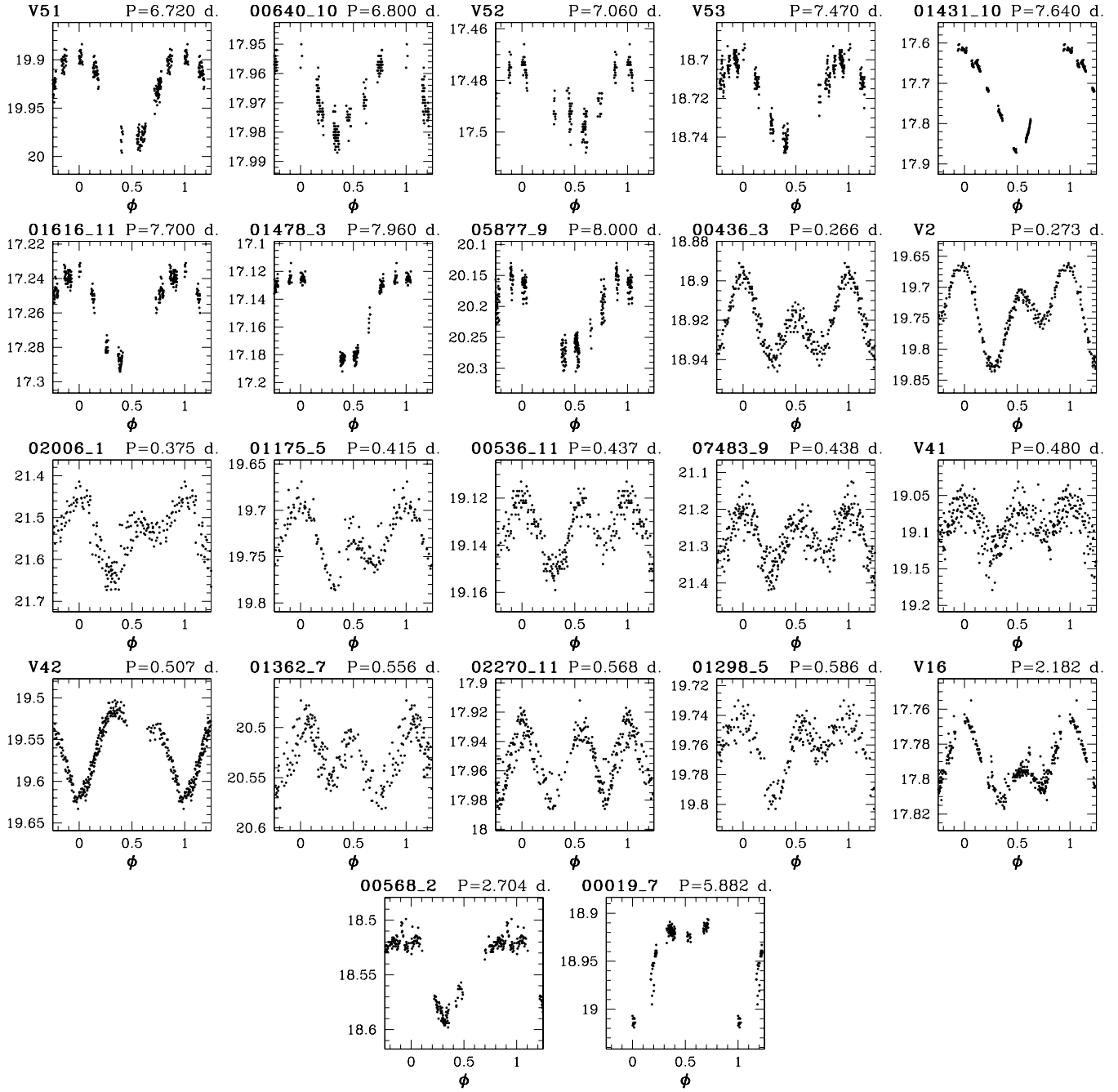


Fig. A.4. Rotational variables with a single-wave (from V51 to 05877_9) and a double-wave light curve.

Table A.6. Long period variable stars (ordered by increasing right ascension).

Star	α_{2000}	δ_{2000}	V	$\langle B - V \rangle$	$\langle V - I \rangle$	Ref.	Memb.	Distance	Star	α_{2000}	δ_{2000}	V	$\langle B - V \rangle$	$\langle V - I \rangle$	Ref.	Memb.	Distance
			[mag]	[mag]	[mag]			[arcmin]				[mag]	[mag]	[mag]			[arcmin]
00091_1	19.323698	37.943716	19.16				nd2	20.2	V90	19.349686	37.746449	18.11	0.86	0.94	k	94	1.9
00143_1	19.323947	37.927971	20.11				nd2	19.5	02011_3	19.349693	37.958382	19.50	1.19	1.16	k	nm	11.3
00250_7	19.324384	37.779393	18.32				nd2	16.8	01908_3	19.349867	37.947132	19.29	1.05	1.09	k	m?	10.6
00326_7	19.324675	37.719342	17.99				nd2	16.9	V91	19.350151	37.811325	18.07	0.83	0.91	k	m?	2.8
00364_7	19.324832	37.798606	20.17				nd2	16.6	07680_9	19.350193	37.718224	18.32	0.89	0.97	k	98	3.5
00377_1	19.325260	38.018518	18.72				nd2	21.9	07914_9	19.350483	37.822048	18.64	1.12	1.27	s	m?	3.5
00466_7	19.325296	37.809032	14.65				nd2	16.3	V100	19.350498	37.761631	17.13	1.02		k	m?	1.8
00435_1	19.325525	37.990790	16.89				nd2	20.7	V31	19.350683	37.785912	17.12	1.00	1.02	k	97	2.1
00537_1	19.325956	38.059293	18.33				nd2	23.3	01344_3	19.350784	37.970558	18.17	1.33	1.48	k	nm	12.1
00552_1	19.325972	37.941670	18.10				nd2	18.7	V62	19.350847	37.731068	19.45	1.02	1.07	k	m?	3.1
00651_7	19.326084	37.647564	16.89				nd2	17.3	01252_3	19.350937	37.911869	19.85	1.55	2.66	k	nm	8.7
00819_7	19.326732	37.764538	18.02				nd2	15.2	08747_9	19.351194	37.651299	21.32	1.50	1.71	s	nm	7.6
00836_7	19.326803	37.684309	19.78				nd2	16.0	00990_3	19.351418	38.014648	17.29				nd2	14.8
00804_1	19.327102	38.039468	21.14				nd2	21.9	V110	19.351603	37.741802	17.75	0.71	0.76	k	25	3.1
00814_1	19.327140	38.035436	20.78				nd2	21.7	09376_9	19.351952	37.831886	18.21	1.00	1.02	k	92	4.6
00973_1	19.327784	37.996820	19.17				nd2	19.7	09611_9	19.352139	37.773365	17.97	0.85	0.91	k	76	2.9
01095_7	19.327905	37.726883	15.41				nd2	14.6	V66	19.352339	37.748669	15.95	1.29	1.39	k	m?	3.3
01145_1	19.328252	38.051636	20.12				nd2	21.8	00038_3	19.352835	37.851254	19.06	0.88	0.97	k	m?	5.9
01382_7	19.329091	37.812623	18.99				nd2	13.7	00176_10	19.353423	37.611797	17.90	1.39	1.59	k	nm	10.3
01536_7	19.329780	37.640689	17.85	0.91		k	nm	15.2	V58	19.354042	37.801240	17.52	0.89	0.94	k	87	4.6
01513_1	19.330106	37.876259	17.18	0.70		k	nm	14.2	00630_10	19.354660	37.738732	18.98	1.27	1.29	k	m?	5.1
01746_7	19.330667	37.812027	18.84	1.08		k	nm	12.6	00670_10	19.354823	37.806999	23.18	-0.40	0.54	s	m?	5.3
01829_7	19.330990	37.707912	15.20	1.31		k	nm	12.7	01536_4	19.355383	37.882149	17.21	1.18	1.29	k	nm	8.4
01873_1	19.331671	37.912256	19.41	0.98		k	nm	14.4	01415_4	19.355972	38.000843	17.60	1.50	1.92	k	nm	14.9
02096_7	19.332013	37.776243	16.79	1.05		k	nm	11.4	01169_10	19.356078	37.634936	15.34	0.88	1.02	k	nm	10.0
02126_7	19.332109	37.673400	19.20	1.38		k	nm	12.8	V55	19.356228	37.841698	16.12	1.48	1.88	k	nm	7.2
02004_1	19.332252	38.055218	19.85				nd2	20.4	01232_10	19.356296	37.664158	19.31	1.41	1.64	k	nm	8.7
02262_7	19.332626	37.658640	17.99	0.77		k	nm	12.9	01225_10	19.356349	37.770012	21.02		2.91	k	nm	5.9
V114	19.333338	37.812103	17.60	1.10	1.15	k	m?	10.7	01279_10	19.356519	37.757845	20.83	1.00	1.22	k	nm	6.1
00285_2	19.334742	38.038967	19.13				nd2	18.6	01210_4	19.356915	37.957123	17.69	0.75	0.86	k	nm	12.8
00404_8	19.335062	37.790737	18.68	0.69		k	nm	9.3	01417_10	19.356934	37.756828	17.03	1.11	1.17	k	nm	6.4
00386_2	19.335152	37.960213	21.51				nd2	14.6	01101_4	19.357428	37.882973	18.25	1.02	1.11	k	nm	9.4
00620_8	19.335981	37.656742	18.99	1.61	2.08	k	nm	11.0	01082_4	19.357555	37.938122	20.49	1.24	1.10	k	nm	12.1
00791_2	19.337513	38.014545	18.01				nd2	16.4	01070_4	19.357592	37.913498	17.53	1.49	2.15	k	nm	10.9
00907_2	19.338146	38.041290	15.62				nd2	17.6	01682_10	19.357705	37.729503	18.40	0.93	0.98	k	m?	7.3
01212_8	19.338499	37.721958	18.45	0.99	1.10	s	nm	7.4	01807_10	19.358104	37.721153	18.17	1.49	2.02	k	nm	7.8
01222_8	19.338552	37.737770	18.26	1.12	1.18	k	nm	7.1	00920_4	19.358349	37.962833	17.65	0.98	1.00	k	nm	13.6
01126_2	19.339148	37.937424	16.93				nd2	11.8	01885_10	19.358407	37.824782	19.23	0.83	0.88	k	nm	8.0
01122_2	19.339149	38.031670	18.55				nd2	16.8	02145_10	19.359033	37.664901	16.66	1.24	1.36	k	nm	10.1
01406_8	19.339247	37.695103	19.03	1.22	1.37	k	nm	7.8	02165_10	19.359100	37.668317	19.60	1.54	2.31	k	nm	10.0
V59	19.339304	37.806061	17.96	1.30	1.42	k	nm	6.6	02250_10	19.359370	37.663215	18.71	0.99	1.12	k	nm	10.4
01179_2	19.339432	37.995293	19.66				nd2	14.7	00717_4	19.359394	37.895435	18.02	1.28	1.42	k	nm	11.0
01622_8	19.340046	37.629841	18.09	1.42	1.64	k	nm	10.2	00718_4	19.359436	37.961086	20.26	1.44	1.67	k	nm	13.9
02022_8	19.341475	37.682644	18.58	1.27	1.44	k	nm	7.1	02268_10	19.359475	37.731544	18.59	0.95	0.99	k	m	8.5
02108_8	19.341743	37.645943	19.50	0.97	1.12	k	nm	8.8	00598_4	19.360041	37.997711	16.73	0.90	1.05	k	nm	16.0
02138_8	19.341864	37.749653	19.68	1.12	1.18	k	m	4.6	00569_4	19.360079	37.848969	19.88	1.23	1.28	k	nm	9.7
02444_8	19.342766	37.810604	18.34	0.93	1.00	k	78	4.4	00538_4	19.360250	37.932350	17.58	0.96	0.99	k	nm	13.0
06098_3	19.343510	38.050224	18.50				nd2	17.0	00422_4	19.360813	37.962696	18.18	1.00	1.12	k	nm	14.6
05998_3	19.343616	37.956688	19.21	1.39	1.52	k	nm	11.5	00381_4	19.360947	37.864788	19.81	1.62	2.35	k	nm	10.7
05951_3	19.343662	37.927708	18.06				nd1	9.9	00313_4	19.361338	37.894558	18.56	0.72	0.79	k	nm	12.0
05938_3	19.343676	37.927959	18.19				nd1	9.9	02898_10	19.361434	37.604020	22.56				nd2	13.9
00510_9	19.343704	37.796719	18.67	0.94	0.98	k	83	3.4	02924_10	19.361641	37.711676	18.04	1.47	1.82	k	nm	10.3
05870_3	19.343727	37.882679	21.96				nd1	7.3	00092_11	19.363431	37.702573	18.52	1.63	1.95	k	nm	11.7
00835_9	19.344023	37.766895	20.02	1.21	1.25	k	m?	2.9	00097_5	19.363811	37.998650	19.70	0.97	0.99	k	nm	17.6
05677_3	19.344053	37.908951	18.83	1.50	1.81	k	nm	8.7	00473_11	19.364836	37.670896	19.83	0.75	0.91	k	nm	13.4
05524_3	19.344362	38.041668	20.16				nd2	16.4	00297_5	19.365023	37.926561	22.15				nd2	15.2
01610_9	19.344818	37.740486	19.09	1.01	1.05	k	m	3.0	00553_11	19.365157	37.749285	16.26	0.92	1.02	k	nm	12.2
05014_3	19.345045	37.876141	16.24	1.06	1.17	k	m?	6.6	00448_5	19.365911	37.852960	17.32				nd2	13.6
V94	19.345139	37.743549	17.54	0.88	0.92	k	90	2.7	00819_11	19.366089	37.737134	18.77				nd2	13.0
V95	19.345295	37.792412	19.16	1.03	1.10	k	93	2.3	00521_5	19.366291	37.911656	17.26				nd2	15.4
04768_3	19.345497	37.987465	19.83	1.16	1.22	k	m?	13.1	00601_5	19.366800	37.992387	17.91				nd2	18.8
04666_3	19.345663	38.023544	15.83				nd2	15.2	01021_11	19.366890	37.806929	17.40				nd2	13.6
02716_9	19.345829	37.651981	17.69	1.45	1.73	k	nm	7.4	00793_5	19.367687	37.917070	18.32				nd2	16.5
V56(=V96)	19.345908	37.763525	17.01	0.95	0.97	k	98	1.6	01304_11	19.367749	37.637939	18.65				nd2	16.2
04392_3	19.345982	37.870571	17.90	0.88	0.92	k	m	6.1	00922_5	19.368542	37.950158	18.62				nd2	18.1
04368_3	19.346024	37.882671	19.62	1.13	1.12	k	m?	6.8	01525_11	19.368695	37.773095	18.81				nd2	14.7
04293_3	19.346100	37.838703	19.46				nd1	4.3	01695_11	19.369359	37.789309	17.96				nd2	15.2
04298_3	19.346115	37.886810	18.35	0.78	0.92	k	nm	7.0	01785_11	19.369770	37.820589	17.13				nd2	15.7

Table A.6. continued.

Star	α_{2000}	δ_{2000}	V	$\langle B - V \rangle$	$\langle V - I \rangle$	Ref.	Memb.	Distance	Star	α_{2000}	δ_{2000}	V	$\langle B - V \rangle$	$\langle V - I \rangle$	Ref.	Memb.	Distance
			[mag]	[mag]	[mag]			[arcmin]				[mag]	[mag]	[mag]			[arcmin]
04160_3	19.346313	37.864944	17.34	1.06	1.11	k	m?	5.7	02010_11	19.370466	37.700018	19.73				nd2	16.5
03987_3	19.346600	37.910511	19.17	1.04	1.10	k	m?	8.4	01245_5	19.370613	37.897333	18.30				nd2	17.7
V75	19.346651	37.766308	17.38	0.94	0.98	s	m	1.0	02401_11	19.371975	37.721131	16.62				nd2	17.3
03687_9	19.346727	37.787651	20.13	1.07	1.45	k	m?	1.3	02419_11	19.371994	37.662943	17.30				nd2	18.2
03859_3	19.346788	37.889477	20.95	1.11	1.85	k	nm	7.1	02550_11	19.372438	37.653960	21.54				nd2	18.7
04133_9	19.347109	37.777020	18.47	0.94	0.98	k	98	0.7	00941_12	19.376714	37.722466	17.77				nd2	20.6
V76(=V85)	19.347192	37.764169	18.19	1.03	1.15	k	97	0.8	01041_12	19.376987	37.656970	17.89				nd2	21.7
V86	19.347258	37.808815	19.44	1.06	1.14	k	83	2.3	01038_12	19.377120	37.779197	20.33				nd2	20.7
V87	19.347996	37.749668	18.12	0.91	0.93	k	98	1.3	01150_12	19.377457	37.669195	17.18				nd2	21.8
05487_9	19.348234	37.677147	18.53	0.93	1.01	k	m?	5.7	01275_12	19.378092	37.727700	20.16				nd2	21.5
05673_9	19.348469	37.793930	20.61	1.29	1.62	k	m?	1.4	01807_12	19.380555	37.832929	18.99				nd2	23.4
05740_9	19.348534	37.808022	17.96	0.93		k	95	2.2	01915_12	19.381010	37.826766	20.20				nd2	23.7
06509_9	19.349110	37.684639	20.79	1.37	1.79	k	m?	5.3	02001_12	19.381172	37.629091	20.49				nd2	25.1
06532_9	19.349180	37.785137	18.01	0.91	0.95	s	m?	1.1	01961_12	19.381188	37.780646	17.87				nd2	23.6
06725_9	19.349329	37.724495	17.77	0.91		k	91	3.0	01968_12	19.381265	37.804920	18.71				nd2	23.7
06796_9	19.349415	37.769268	18.46	0.92	1.04	k	92	1.0	02176_12	19.381966	37.690587	19.60				nd2	24.6